Check for updates

RESEARCH ARTICLE

Risk assessment for Na-Zn liquid metal batteries

[version 1; peer review: 2 approved with reservations]

Norbert Weber, Carolina Duczek, Gleidys Monrrabal, William Nash, Martins Sarma, Tom Weier

Helmholtz-Zentrum Dresden-Rossendorf, Bautzner Landstr. 400, 01328 Dresden, Germany

v1 **First published:** 25 Oct 2024, **4**:236
https://doi.org/10.12688/openreseurope.17733.1
Latest published: 25 Oct 2024, **4**:236
https://doi.org/10.12688/openreseurope.17733.1

Abstract

Background

Na-Zn liquid metal batteries, which operate at 600 °C, have recently been proposed as inexpensive stationary energy storage devices. As with any other electrochemical cell, their fabrication and operation involves certain risks, which need to be well understood in order to be minimised.

Methods

A risk assessment according to ISO 12100 is performed at the cell level for operating Na-Zn cells in the laboratory environment. Hazard identification and risk evaluation are systematically addressed, including a thorough literature review, theoretical calculations and selected experiments.

Results

Cell overpressure is found to be one of the main risks – and might be caused either by mistakes in battery production (humidity) or operation (over-charge/discharge). In terms of cell housing, the weakest component is clearly the feedthrough. Its failure might lead to the release of hazardous aerosols to the environment. In this context, the candidate electrolyte components LiCl and BaCl2 are especially dangerous, and should therefore be reduced or avoided if possible.

Conclusions

Overall, Na-Zn cells are expected to reach a very high safety level, similar to state-of-the-art ZEBRA technology, as they are not prone to

Open Peer Review

Approval Status ? ?

	1	2
version 1 25 Oct 2024	? view	? view

1. **Farooq Ahmad**, nstitute of Molecular Physics Polish Academy of Sciences, Poznań, Poland

2. **Binghe Liu**, Chongqing University, Chongqing, China
Yue Liu, Chongqing University (Ringgold ID: 47913), Chongqing, China

Any reports and responses or comments on the article can be found at the end of the article.

thermal runaway. However, considering the still low TRL level and open questions concerning the durability of certain parts of their housing, the batteries should preferably be operated under a fume hood.

Keywords
battery safety, risk assessment, liquid metal battery, molten salt battery, sodium zinc battery



This article is included in the Horizon 2020 gateway.

Corresponding author: Norbert Weber (norbert.weber@hzdr.de)

Author roles: Weber N: Conceptualization, Funding Acquisition, Investigation, Methodology, Project Administration, Supervision, Visualization, Writing – Original Draft Preparation, Writing – Review & Editing; **Duczek C**: Investigation, Methodology, Writing – Review & Editing; **Monrrabal G**: Investigation, Writing – Original Draft Preparation, Writing – Review & Editing; **Nash W**: Conceptualization, Investigation, Writing – Original Draft Preparation, Writing – Review & Editing; **Sarma M**: Conceptualization, Formal Analysis, Investigation, Methodology, Visualization, Writing – Review & Editing; **Weier T**: Funding Acquisition, Investigation, Methodology, Project Administration, Supervision, Writing – Review & Editing

Competing interests: No competing interests were disclosed.

Grant information: This project has received funding from the European Union's Horizon 2020 research and innovation program under grant agreement No 963599 (Sodium-Zinc molten salt batteries for low-cost stationary storage [SOLSTICE]).
The funders had no role in study design, data collection and analysis, decision to publish, or preparation of the manuscript.

Copyright: © 2024 Weber N *et al*. This is an open access article distributed under the terms of the Creative Commons Attribution License , which permits unrestricted use, distribution, and reproduction in any medium, provided the original work is properly cited.

How to cite this article: Weber N, Duczek C, Monrrabal G *et al.* **Risk assessment for Na-Zn liquid metal batteries [version 1; peer review: 2 approved with reservations]** Open Research Europe 2024, **4**:236 https://doi.org/10.12688/openreseurope.17733.1

First published: 25 Oct 2024, **4**:236 https://doi.org/10.12688/openreseurope.17733.1

1 Introduction

A lithium battery bursting into flames is probably the first image one has in mind when thinking of battery safety[1,2]. Such thermal runaway is not limited to Li-ion cells, but can of course take place in other chemistries, such as Ni-Cd or lead acid batteries, too[3]. While fire and explosion are the most obvious consequences, invisible toxic gases such as CO, NO, HF, SO_2 and HCl for Li-ion cells, or HS, arsine and stibine for lead acid batteries, might also be released[3].

High-temperature batteries, which operate above 100 °C by definition[4], are only partly susceptible to thermal runaway. A failure in the solid electrolyte of ZEBRA[5,6] or Na-S cells[7] will lead to short-circuit and mixing of the anode[i] and cathode compartments. Luckily, this is safe for ZEBRA batteries, as the reaction of Na (anode) with the catholyte ($NaAlCl_4$) leads to the formation of solid aluminium, cell freezing and a low-impedance permanent short-circuit[8–13]. However, shorting a Na-S cell will lead to the formation of strongly corrosive sodium polysulphides and fast temperature increase, which can easily destroy the cell housing or seal. Much work in the past has therefore been invested to design Na-S cells inherently safe to prevent propagation of one cell's failure to others[14,15].

While safety analysis has been performed for all battery chemistries mentioned above, to our best knowledge no risk assessment has been published for Liquid Metal Batteries (LMBs)[16]. Such cells employ a molten salt electrolyte, which has motivated much fluid dynamic research with the idea in mind that strong flow could easily short-circuit thin electrolyte layers[17,18]. Short-circuits have repeatedly been observed in LMB experiments[19–25] leading even to salt evaporation[20]. It is therefore the aim of this work to perform a thorough risk assessment of a liquid metal battery using the example of a Na-Zn cell operating at 600 °C[26–28].

With regards to risk assessments, safety standards are very important as they provide guidance to identify and avoid possible risks. Of course, they depend on the country and many different standards exist. In our opinion the following are most relevant for designing safe batteries (see also Table 13):

- UL 9540 provides safety requirements as well as safety tests for complete *energy storage systems* – including thermal, mechanical and chemical storage[29]
- IEC 62984-2 describes safety rules as well as safety tests specifically for *high-temperature batteries* from an *electrotechnical perspective*[30]
- UL 1973 is the safety standard for *stationary batteries* – including rules for construction, battery design, software, communication systems, fire protection as well as safety tests including abuse[31]
- UL 9540A provides tests for *thermal runaway* of battery energy storage systems – from cell to module to unit – including extreme abuse[32]

[i] We follow here the convention of using the terms 'anode' and 'cathode' for the negative and positive electrodes respectively.

While the standards UL 9540, IEC 62984-2 and UL 1973 must be met by any high-temperature stationary energy storage systems, the UL 9540A thermal runaway certification is harder to achieve. ZEBRA batteries sold by FZSoNick and Na-S cells from NGK comply with the latter, while Li-ion batteries usually do not[33]. This additional certification is the reason that ZEBRA batteries are especially popular in applications for which fire safety is critical.

2 Methods

This risk assessment follows the method defined by ISO 12100 and ISO/TR 14121-2[34,35]. Where applicable, the following standards and regulations are considered:

- ISO standards (International Organisation for Standardisation)
- EN standards (European Standards)
- IEC standards (International Electrotechnical Commission)
- UL standards (Underwriters Laboratories)
- IEEE standards (Institute of Electrical and Electronics Engineers)
- Directives of the European Parliament and of the Council

As illustrated in Figure 1, the risk assessment starts with a hazard identification. Using a bottom-up approach, i.e. considering all possible ways that something can go wrong, and following the systematic methodology suggested in ISO 12100[34], possible hazards are identified and listed in an Excel spreadsheet.

The associated risk is estimated using a numerical approach by evaluating the severity score (SS), which describes the severity and extent of harm, and the probability score (PS) which accounts for the duration and frequency of harm, the probability of an event occurring and the possibility of avoiding it[35]. The sum of both gives the risk score (RS) – for the definitions, see Table 1.

After evaluating each individual risk, suitable risk reduction methods are identified[34,35]. Generally, inherently safe designs

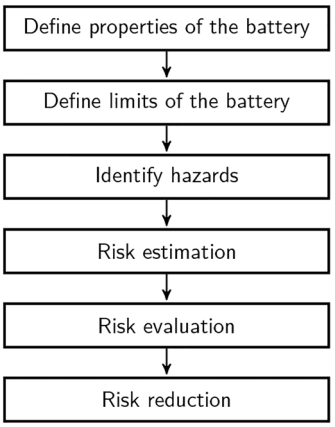

Figure 1. Steps of the risk assessment.

Table 1. Definitions for risk estimation, following ISO/TR 14121-2[35].

severity score (SS)		probability score (PS)		risk score (RS = SS + PS)	
%	definition	%	definition	%	definition
SS ≤ 29	minor	PS ≤ 29	remote	RS ≤ 89	negligible
30 ≤ SS ≤ 89	moderate	30 ≤ PS ≤ 69	unlikely	90 ≤ RS ≤ 119	low
90 ≤ SS ≤ 99	serious	70 ≤ PS ≤ 99	likely	120 ≤ RS ≤ 159	medium
SS = 100	catastrophic	PS = 100	very likely	RS ≥ 160	high

are always preferred. Only if this is not possible, safeguarding measures are suggested, or if unfeasible, information for safe use is provided. The Excel table containing the overview of the risk assessment can be found in Section 6.2; the details are discussed in the following.

3 Scope of the study

The life of a battery involves many phases, starting from mining of the raw materials and ending with recycling – as illustrated in Figure 2. Considering that – with the exception of AMBRI[ii] – LMBs are not commercially available, but were mostly investigated in the laboratory, we limit the risk assessment to the use phase of experimental batteries. The cells are typically assembled in a glovebox and operated in a simple laboratory furnace.

3.1 Battery design and operation

Figure 3 shows the cell assembly, Table 2 describes the single parts[28] and Section 6 provides all details of the cell design. The housing is made of welded standard components, and is closed using a CF40 vacuum flange with Cu sealing. A tube in the lid allows connecting a pressure sensor and introducing thermocouples into the cell. Current is supplied via two feedthroughs, which are connected via barrel connectors to the Mo (or W) current collectors. The active material is contained in an alumina crucible, with a ceramic sheath insulating anode and cathode. The molten salt consists usually of $CaCl_2$-NaCl, but $BaCl_2$, KCl, LiCl and $SrCl_2$ might be added, too, in order to improve the electrolyte's properties. In order to reduce self-discharge, it is split into an upper and lower compartment using a porous diaphragm, which is hold in place by a thin alumina cylinder. The cell is filled in discharged state with Zn metal and $CaCl_2$-NaCl, which reacts according to the equation

$$2\,Na + ZnCl_2 \leftrightarrow 2\,NaCl + Zn \qquad (1)$$

to Na metal and $ZnCl_2$ at charge.

[ii] https://ambri.com/

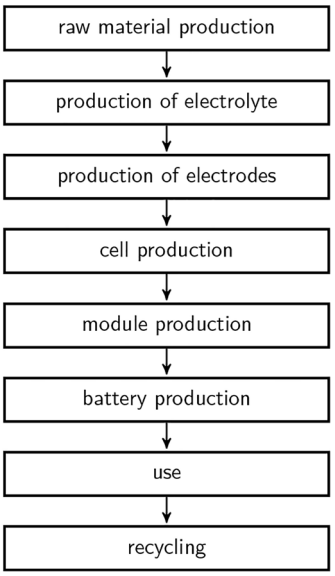

Figure 2. Phases of life of a battery.

3.2 Operational limits

The cell needs to be operated within certain limits, which are summarised in Table 3 and are explained in the following.

- Temperature: the minimum temperature is defined by solidification of the salt; the maximum temperature by the stability of the feedthroughs.
- Open-circuit potential (OCV): Discharged cells in experiments typically exhibit 1.2 V, while the maximum predicted cell potential is 1.8 V when using the standard potentials from Hamer *et al.*[36] and Temkin's model for the $ZnCl_2$ concentration in the molten salt[37,38]. Experimentally observed OCVs are typically in the range 1.6–1.7 V.
- Depth of discharge (DoD): the depth of discharge can be calculated from the phase diagram, shown in Figure 4. The enrichment in $CaCl_2$ upon charging arises because two moles of NaCl are required to

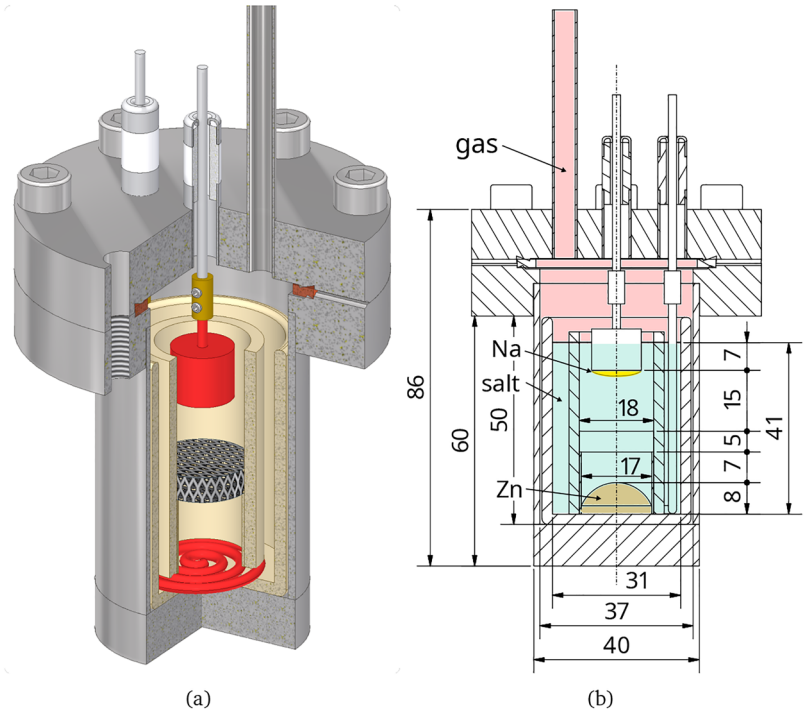

Figure 3. Cell design and main dimensions[28].

Table 2. Parts of the ALB and their properties[28]. Densities are given for room temperature, and heat capacities for 600 °C.

part	quantity	specification	density	mass	c_p	comment
			g/cm³	g	J/(kg K)	
housing	1	1.4306 (X2CrNi19-11)	7.9[39]	320	600[39]	values for 1.4301
lid	1	1.4306 (X2CrNi19-11)	7.9[39]	335	600[39]	values for 1.4301
screws	6	1.4980	7.9[39]	7	600[39]	values for 1.4301
tube	1	1.4306 (X2CrNi19-11)	7.9[39]	19	600[39]	values for 1.4301
bottom plate	1	1.4306 (X2CrNi19-11)	7.9[39]	107	600[39]	values for 1.4301
sealing ring	1	Cu	9.0[40]	11	438[41]	
diaphragm	1	alumina foam	3.8[42]	1	1200[43]	porosity 0.9[44]
crucible	1	Al_2O_3 > 99.5 %	3.8[42]	59	1200[43]	
sleeve	1	Al_2O_3 > 99.5 %	3.8[42]	28	1200[43]	
diaphragm support	1	Al_2O_3 > 99.5 %	3.8[42]	2	1200[43]	
barrel connector	2	Mo	10.2[40]	2	290[41]	
screws barrel connector	4	A4 (1.4401)	7.9[39]	0.1	600[39]	values for 1.4301
anode current collector	1	Mo	10.2[40]	12	290[41]	
cathode current collector	1	Mo	10.2[40]	5	290[41]	
Zn		Zn	6.4[45]	25	481[46]	
salt ($CaCl_2$:NaCl)		44:56 mol% 60:40 wt%	1.9[47]	32	864[41]	weighted by mass σ = 1.38 S/cm[47]
feedthrough (2 pieces)						

part	quantity	specification	density	mass	c_p	comment
			g/cm³	g	J/(kg K)	
ceramic ring	1	alumina	3.8[42]	2	1200[43]	
lower collar	1	Invar 42, 1.3917	8.1[48]	1	689[41]	c_p weighted by mass
upper collar	1	Invar 42, 1.3917	8.1[48]	1	689[41]	c_p weighted by mass
wire	1	Invar 42, 1.3917	8.1[48]	1	689[41]	c_p weighted by mass
braze 1	1	Ni	-	0.1	535[41]	
braze 2	1	Au	-	0.4	141[41]	
sum/mean				1013	653	c_p weighted by mass

Table 3. Operation parameters and limits of a Na-Zn LMB based on the Zn and salt amounts given in Table 2. The values are mostly estimates, based on the experience of the authors.

property	unit	typical value	min	max	comment
Temperature	°C	600	550	600	
OCV	V	1.6-1.7	1.2	1.8	depends on exact salt
Current density	mA/cm²	100	0	350	
Cell current	A	0.25	0	1	
Overall efficiency	%	75	60	90	estimated
Depth of discharge	%			45	until salt solidifies
Capacity	Ah	0.5			depends on catholyte volume
Discharge rate		C/2	C/16	1C	
Energy content	Wh	0.9			

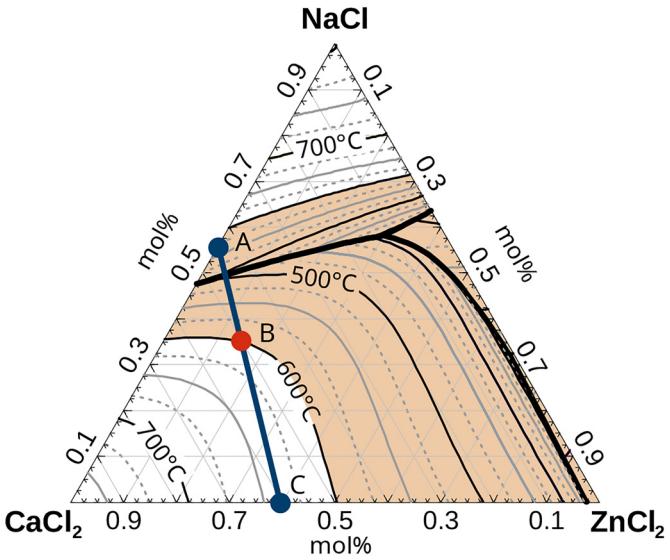

Figure 4. Phase diagram of $CaCl_2$-NaCl-$ZnCl_2$ and discharge line[49]. The concentration at point A (discharged) is 44:56 mol% $CaCl_2$:NaCl, at point B (solidification) 50:35:15 mol% $CaCl_2$:NaCl:$ZnCl_2$ and at C (fully charged) 61:39 $CaCl_2$:$ZnCl_2$. The shaded area shows the compositions where the electrolyte is liquid below 600 °C.

produce one mole of $ZnCl_2$. Assuming that all of the NaCl in the discharged cell (salt composition 44:56 mol% $CaCl_2$-NaCl) reacts to form $ZnCl_2$, a composition of 61:39 mol% $CaCl_2$-$ZnCl_2$ would result (0.5 * 56/(0.5 * 56 + 44) mol% $ZnCl_2$). At an operating temperature of 600 °C, the solidus line is encountered at a salt composition of 50:35:15 mol% $CaCl_2$-NaCl-$ZnCl_2$. As two moles of NaCl react to one mole of $ZnCl_2$ during discharge, the total amount of substance does not stay constant, when following the discharge line in the phase diagram. Assuming that the cell is filled with 100 mol salt, 44 mol thereof being $CaCl_2$, 44/50 = 88 mol of salt will remain upon solidification. This results in 0.35 · 88 = 31 mol NaCl left, or 31/56 = 55 mol% left and therefore in a DoD of 45 %.

- Operation potential window: at potentials above 2.5 V the cathode current collector could corrode, and at potentials below -0.6 V the anode current collector, see Table 16.

- Energy density: the charge released when producing one mole of Zn is $Q = 2F = 53.6$ Ah because two electrons are involved in the reaction. The cell voltage is assumed to be 1.8 V as this is the maximum possible value. The mass necessary to produce one mole of Zn is given by molar masses of Na and $ZnCl_2$ as $m = 2{\cdot}23\,g + 136.3\,g = 182.3\,g$. The theoretical energy density is then $w = Q \cdot U/m = 529$ Wh/kg.

- Capacity: capacity is computed such that all NaCl is consumed until solidification (see DoD) and that only the volume below the diaphragm and within the diaphragm support is taken – see Figure 3. This gives 2.65 cm^3.

- Current density: the typical current density is calculated such that it allows for operating at a voltage efficiency of 75 % – for the salt conductivity, see Table 2. The Zn surface area is used to compute the current density.

- Operators: the cell is only operated by trained and skilled persons.

- Mode of operation: the operation can be divided into heat-up, open circuit, charge, discharge and cool-down, further maintenance (putting cell in furnace, taking it out, connecting it), malfunctions (short-circuit, failure of housing, potentiostat failure, heating system failure) and misuse (short-circuit, overcharge, ...).

- Environment: the cell will be operated indoors at normal air humidity, without exposure to water. The temperature of the surrounding laboratory environment will remain between 0 and 40 °C.

4 Results

4.1 Intrinsic material hazards

Na-Zn LMBs employ molten metals, various salts and ceramics which may, together with their corrosion products, present certain intrinsic material hazards. Table 4 gives an overview.

4.1.1 Metals. While Zn metal is generally safe (although Zn vapour should not be inhaled), Na presents several risks. Cold metallic Na is corrosive to human tissue, and causes severe burns to the eyes, skin, lungs and the respiratory system[50–52]. Splashes in the eye are especially dangerous and can cause blindness[51]. Na droplets might burn even at 125 °C; thus a fire risk exists as soon as Na is in contact with air[53,54]. The speed at which a Na fire spreads depends crucially on its surface area, with the flames producing Na_2O and Na_2O_2 of which 40 % end up as aerosols[53]. These oxides react gradually to form NaOH with air humidity and finally to Na_2CO_3 with carbon dioxide[53]. Na reacts directly with moisture, producing NaOH and hydrogen[53]. The latter may ignite spontaneously[55], especially above 560 °C[53]. Air-hydrogen mixtures are flammable or explosive between 4 and 77 vol%[3,50,56,57]; however, with the necessary safety factors, often 1 or 2 vol% are mentioned as lower limits. Na fires can be extinguished by dry sand, cement or special metal-fire extinguishers; water and CO_2 are very dangerous and must be avoided[58].

Depending on the salt composition, other alkali or alkaline earth metals such as Ba, Ca, Li, K or Sr may be codeposited at the anode during charging. These should be treated in the same way as Na, as all of them may react to form appreciably corrosive oxides/hydroxides and hydrogen[50]. Special care is required when handling K as it reacts with air to form highly explosive peroxides[50]. The yellow crust on its surface can be detonated simply by cutting it with a knife[59]. Finally, Ba is highly toxic and its reaction products can even be absorbed through the skin[50]. Ba ions act as muscle stimulants and can cause death due to ventricular fibrillation[59].

4.1.2 Molten salts. The hazard presented by the electrolyte depends strongly on its chemical composition:

- $BaCl_2$ is highly toxic and damages muscles, intestine and heart[51]. Its main exposure route is via the lungs[50].

- $CaCl_2$ causes irritation of the skin and eyes, but is otherwise relatively safe[50].

- KCl is not considered a hazardous substance[50].

- LiCl is irritating for skin and eyes and toxic if swallowed[50]. Its reproductive toxicity is currently under discussion, with the classification cat. 1A proposed[60].

- NaCl is not considered a hazardous substance[50].

- $SrCl_2$ is classified as eye damaging but otherwise comparably safe.

- $ZnCl_2$ causes strong irritation of the eyes, skin, and respiratory system, with aqueous solutions being corrosive. Exposure is possible via the skin or when swallowed, leading to damage to the intestine, kidneys and heart. $ZnCl_2$ produces HCl when heated in air and is very toxic to aquatic life with long-lasting effects[50,51].

4.1.3 Corrosion products. It is difficult to predict which exact corrosion products may appear. However, based on the components of the housing, the following should be considered:

Table 4. Hazards of materials and corrosion products. The numbers in the table specify the GHS hazard category[61] and are taken from GESTIS[50] and various material data sheets.

	skin			eye		respiratory sensitisation	toxic				CMR							
	irritating	corrosive	sensitisation	irritating	damage		skin contact	swallowed	inhaled	damage to organs	germ cell mutagenicity	carcinogen	reproductive toxicity	corrosive to metals	flammable solid	reacts with water	toxic to aquatic life (acute)	toxic to aquatic life (chronic)
Na		1B														1		
Zn																		
Ba		1B			1			3							1	1		
Ca																2		
K		1B			1											1		
Li		1B			1											1		
Sr	2															1		
$BaCl_2$				2				3	4									
$CaCl_2$				2														
KCl																		
LiCl	2			2				4					(1A)					
NaCl																		
$SrCl_2$					1													
$ZnCl_2$		1B						4									1	1
Na_2O		1B																
NaOH		1A		1										1				
ZnO																	1	1
$Zn(OH)_2$																	1	2
AgCl														1			1	1
$AuCl_3$		1B	1															
Cl_2	2			2					2	3							1	1
$CrCl_2$	2			2				4		3								
$CrCl_3$			1					4						1				2
CuCl	2				1		4	4									1	1
$CuCl_2$	2				1		4	4						1			1	1
$FeCl_2$		1B			1			4						1				
$FeCl_3$	2		1		1			4						1				
HCl		1A			1				3									
$MoCl_3$	2			2						3								
$MoCl_5$		1B																
$NiCl_2$	2		1			1		3	3	1	2	1A	1B				1	1
WCl_6		1B			1			4										
PH_3		1B			1				1								1	
fibres												1B						

- active metals: NaOH, Na_2O, $Zn(OH)_2$ and ZnO might result from humidity
- feedthrough: Au or Ag might dissolve in small amounts from the feedthrough braze
- HCl and Cl_2 gas may evolve due to hydrolysis or salt decomposition
- sealing: Cu ions might be present
- current collector: Mo or W reaction products might appear
- housing: Fe, Cr and Ni reaction products may dissolve

Table 4 gives a selection of possible corrosion products. It is obvious that corrosion products pose rather greater hazards than the active materials. Many of them are corrosive and toxic, including to aqueous life, and some are even carcinogenic.

4.1.4 Ceramics. Binders and additives of ceramics are often $AlPO_4$-based. The phosphorous can be reduced by certain alkali and earth alkaline metals to form metal phosphides. These may react with water to form highly toxic phosphine (PH_3) gas, which is absorbed very fast in the lungs. Breathing such gas for 5 minutes at a concentration of 1000 ppm is lethal[50,62,63]. In certain cases, ceramic Al_2O_3 fibre material is used as a diaphragm. When entering the lungs, such fibres can cause cancer, with the probability being determined by the dose of exposure, dimensions of the fibres, and their biopersistence. Fibres with a diameter $< 3\,\mu$m, a length $> 5\,\mu$m and a length-to-diameter ratio of $> 3{:}1$ are considered carcinogenic[64]. Further, Al_2O_3 is considered very biopersistent, and therefore needs to be classified as carcinogenic cat. 1B[50].

4.1.5 Recommendations. Battery safety can be increased significantly by avoiding $BaCl_2$ and ceramics which contain $AlPO_4$-based binders. When disassembling and cleaning cells, this work should only be performed in a fume hood while wearing gloves and eye protection. In case of accidents, the main exposure to toxic substances is probably via the lungs due to vapours, aerosols and possibly PH_3. Further, hydrogen might be released. If it cannot be assured that the housing is hermetically sealed under all circumstances, the cells must be operated inside a fume hood to evacuate toxic or explosive gases[3]. Hydrogen traps need to be avoided[3]. Finally, a second crucible or absorption material around the cell might be useful to catch up spills[65].

4.2 Electrical hazards

Typical electrical hazards include:

- Short circuit: any fast discharge may lead to cell heating and pressure buildup, as explained in Section 4.5.5. Reasons for a short circuit might be abuse, a power outage, deposition of Na vapour on a feedthrough, internal self-discharge, Zn deposition or any other internal mutual metallic contact. Short circuits cannot be safely excluded.
- Failure of pressure sensor: if used to monitor battery safety, the system should shut off if the pressure sensor fails.
- Failure of heating system: if a thermocouple or heat controller breaks, the heating system must switch off. Thermocouples need to be fixed safely such that they cannot be removed accidentally. If necessary, a second heat controller for safety shutdown might be installed.
- Overcharge or -discharge: too high or too low cell potentials may lead to current collector corrosion and salt decomposition. The latter may increase the internal pressure considerably, as explained in Section 4.5.4 and must absolutely be avoided. The corrosion potentials for various current collector materials are given in Table 16, the decomposition potentials of the salts in Table 14.

4.3 Thermal hazards

Thermal hazards include mainly

- overheating, which might be caused by broken or removed thermocouples or failure of heat control
- external fire, leading to overpressure and air corrosion as explained in Section 4.5.1 and Section 4.6.1
- skin burns, which may happen if parts with a temperature above 55–65 °C are touched, as shown in Figure 5

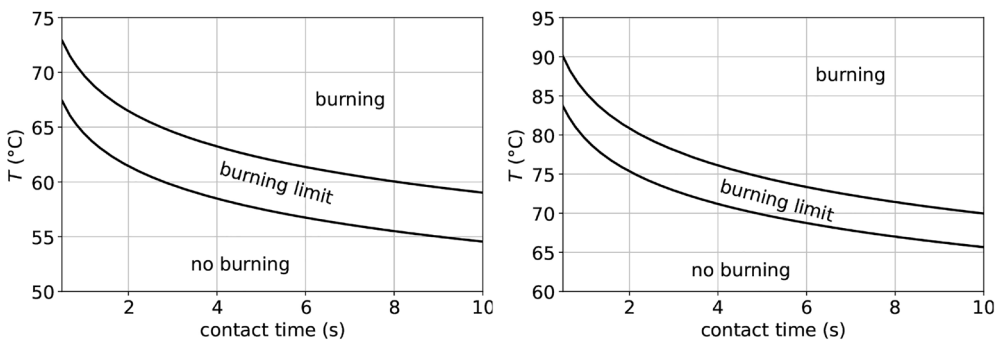

(a) metals (b) ceramics

Figure 5. Burn threshold of metals (**a**) and ceramics (**b**)[66].

4.4 Humidity and salt drying

Humidity is problematic because it may increase cell pressure and induce corrosion. Most salts are appreciably hygroscopic; the latter being defined as the ability of a material to take up water from the environment by adsorption, absorption or capillary action[67,68]. Effective procedures from drying salts are described in the foregoing. Good reviews on general approaches to salt drying are also available[69,70].

The most typical reactions of water with chloride salts are the formation of[69]

- hydrates, e.g. $CaCl_2 + H_2O \longrightarrow CaCl_2 \cdot H_2O$,
- hydroxides due to hydrolysis, e.g. $ZnCl_2 + 2\ H_2O \longrightarrow Zn(OH)_2 + 2\ HCl$,
- oxides due to hydrolysis, e.g. $ZnCl_2 + H_2O \longrightarrow ZnO + 2\ HCl$ and
- hydroxides from oxides, e.g. $CaO + H_2O \longrightarrow Ca(OH)_2$,

which can lead to the formation of hydrogen and contamination of the melt with corrosive O^{2-}, OH^-, Cl^- or H^+ ions. The simplest approach to purifying salts is heating under vacuum. While slightly hydrated salts such as KCl and NaCl can easily be vacuum dried without precautions, care must be taken with others because of hydrolysis reactions[71]. Suitable drying temperatures are best obtained from thermogravimetric analysis (TGA) experiments, salt-water phase diagrams or other suitable literature. Salts which undergo hydrolysis should first be dried in vacuum at low temperature before rising it slowly[69,70]. In order to speed up the process regular purging with inert gas is recommended[71,72]. The achievable vacuum pressure is a measure of the success of the drying procedure.

Salts for which hydrolysis cannot be avoided need to be melted under HCl, and HCl or Cl_2 should be bubbled through this melt to remove oxides/hydroxides[70,71]. This approach does not eliminate the need for vacuum drying. Alternatively, sublimation or distillation may be used although they are rather costly[70].

Barium chloride is hygroscopic and is stable as a dihydrate in contact with air[50,59,73–76]. The water-$BaCl_2$ phase diagram[77] predicts di-hydrate decomposition at 102 °C[77–79], mono-hydrate decomposition at 145 °C[77] and hemi-hydrate decomposition at 167 °C[77,78] at ambient pressure; at 0.1 mbar it can even be fully dried at room temperature. TGA experiments show water loss between 60 and 150 °C; heating to 160 °C is claimed to be sufficient for drying[80]. The dehydration-rehydration process is claimed to be fully reversible[81], but information on hydrolysis is limited[82–84]. At least above 900 °C, hydrolysis has been demonstrated experimentally[83,85] and is also predicted by HSC[41].

Calcium chloride is very hygroscopic[50,59,74]; its phase diagram has been investigated several times[86–91]. $CaCl_2$ can exist as 1/3, mono-, di-, tetra- and hexahydrate[50,92–95]. Smith *et al.* give an excellent overview on drying $CaCl_2$[96]. At ambient pressure, $CaCl_2$-hexahydrate reacts to tetra-, di- and anhydrate and liquid water at 30[97], 45 and 175 °C[59,73–75,98]. However, the dehydration steps and phases depend much on pressure – and in certain cases higher temperature up to approx. 300 °C might be required[94,99]. Further, hydrolysis has occasionally been observed at 380 °C[100,101] – and often at higher temperatures above 600 °C[84,102–104]. Such reactions produce CaO above 400–450 °C[105,106]; at lower temperature, $Ca(OH)_2$ might be more stable. Purifying $CaCl_2$ under vacuum for one week at 100 °C, followed by another week at 225 °C, leads to a contamination of 0.3 wt% H_2O[107], which is equivalent to a more sophisticated purging with HCl at 850 °C under vacuum.

Sodium chloride is only slightly hygroscopic[74]. While mined salt contains up to 0.4 wt% humidity, NaCl does not form hydrates but only adsorbs humidity on the surface[96]. Water-NaCl phase diagrams do exist but focus often on the NaCl-solubility[49,88,108]. Smith *et al.* thoroughly reviewed the drying procedure of NaCl suggesting that drying at 400 °C under vacuum leads to complete water removal[96]. Wang *et al.* found that NaCl contained initially 0.026 % humidity and that complete drying took approx. 12 h at 120 °C[109]. Hydrolysis of NaCl has been investigated repeatedly, and might occur at 450 °C. However, when dried under inert gas, it is considered negligible[96,110–112].

Lithium chloride is extremely hygroscopic[98,113]. Although several hydrates are known, only the monohydrate is relevant as the others only occur below 0 °C[113,114]. Phase diagrams are given by various authors[91,114–116] – see also the references therein. In contact with air, LiCl forms a surface layer of $LiCl \cdot H_2O$ (2.55 % water)[117]. TGA measurements show that drying occurs in two steps between 99–110 and 160–186 °C[118] or according to other authors at 80 °C and the rest between 96 and 175 °C[80]. Hydrolysis has been observed at 390–500 °C[69,72,119], with increasing propensity near the melting point around 600 °C[112,117,119,120]. According to Smirnov *et al.*, hydrolysis produces comparable amounts of oxide and hydroxide[110]. Drying has been shown to be a slow process: vacuum and flushing three times with inert gas needed 40 h at 25 °C, and 20 h at 100 °C to achieve a pressure of 133 Pa[72]. Swain *et al.* carefully reviewed possible drying procedures suggesting that heating to 300 and 500 °C for more than one week under vacuum yields similar purity as using HCl[121]. Other authors suggest based on TGA measurements a temperature of 450 °C under vacuum[72] or 480 °C – 500 °C followed by fusion under vacuum and if possible under anhydrous HCl[120] or Cl_2[96].

Potassium chloride is only slightly hygroscopic, adsorbing water on its surface if humidity surpasses 66 % relative humidity[96,98]. Water-KCl phase diagrams are available[49,88,122]; a good overview on drying is provided by Smith *et al.*[96]. TGA measurements have shown that KCl looses water at 219 °C[80,96]. Hydrolysis can theoretically happen, and has been measured at temperatures as low as 500 °C. However, it is negligible if heated under protective gas[72,110,111,123]. According to Wang

et al., KCl drying required 30 h at 120 °C to remove the 0.03 % water originally present. Typically, heating to 300–400 °C under vacuum with regular flushing with inert gas is the recommended drying procedure[96].

Strontium chloride is hygroscopic, forming hexa-, di-, mono- and hemihydrates[50,73,76,124,125] according to the phase diagram[124,126]. Dehydration under a humid atmosphere proceeds step wise from the hexa- to the di- to the mono-hydrate, from 61–320 °C[98,127]. The exact transformation temperatures depend very much on air moisture – which is the reason why many authors give different values[126–128]. In dry air, only the mono-hydrate is stable[126] and forms the anhydrate at 37 °C[126]. Hydrolysis can be expected especially for the higher hydrates and higher temperature[82,84] and has been shown to occur at 935 °C[85].

Zinc chloride is the most practically challenging of all the salts considered. It is strongly hygroscopic[50,75,95,98,129] and many hydrates are known, including 1.33, 2.5, 3 and 4.5-hydrate[95,129–133]. As can be seen in the phase diagram, dewatering happens in five steps[95,130]. All water is not removed until $ZnCl_2$ is heated above its melting point; the last 0.1 % disappears above 310 °C and is fully lost at 350 °C[130,134]. Threlfall claim that $ZnCl_2$ contains water even up to its boiling point[135].

Hydrolysis of $ZnCl_2$ has often been studied and is as complex as dehydration. It is well known that it depends on the exact salt mixture and that ZnO can limit HCl formation. Depending on the exact conditions, hydrolysis has been observed to set in at temperatures of 160–340 °C[130,136–139]. Giving a thorough overview on the purification of $ZnCl_2$, Hamilton states that the degree of hydrolysis is low[139]. His drying procedure is similar to the one recommended by other authors[140,141], and consists of: vacuum drying for 4–5 days until pressure decreases to $5 \cdot 10^{-3}$ torr; heating to 250 °C for several days until the same pressure is obtained; flushing with HCl while heating to 350 °C; further bubbling with HCl for 5 h; and finally, flushing with dry Ar for 5 h.

Recommendations Salt drying is a mass transfer controlled process. A large surface area of the material, for example as powder, and regular flushing with inert gas is therefore useful. Drying should be performed under vacuum and for sufficient time – as rule of thumb for at least one day, but better a week. Salts should be dried separately, especially those where hydrolysis can be expected. The exact drying procedure, including heating speed and temperature steps, need to be adjusted for the specific salt – based on scientific information such as phase diagrams, TGA measurements or similar. Salts which tend to undergo hydrolysis are generally best predried at room temperature before increasing temperature slowly. In case of very challenging salts such as $ZnCl_2$, purging of the melt with HCl or Cl_2 might be required to remove all moisture.

4.5 Pressure buildup

Pressure buildup in LMBs can have different causes and may potentially be dangerous. The European Pressure Equipment Directive 2014/68/EU provides a regulatory framework to design safe pressure devices[142]. As the volume of our cell is below 1 l and the expected maximum pressure below 200 bar, it does not directly apply.

4.5.1 Heating. Pressure buildup during heating can be adequately approximated by the ideal gas law as[40]

$$pV = nRT \tag{2}$$

with the temperature T in K, the amount of substance n, the gas constant R and cell volume V. As shown in Table 5, this may lead to an overpressure of 2 bar at normal operation. Even a temperature increase to 900 °C would add only one bar more.

Figure 6 shows the measured cell pressure within a battery during heat-up. The slight pressure over-estimation can be attributed to the presence of the pressure-sensor tube (see Figure 3), which encloses a significant volume of gas with a lower temperature than the gas in the main body of the cell (tube dimensions: 300 mm length, 4 mm internal diameter). However, overall the experimental and theoretical curve match well, and do – most importantly – not show evidence of additional pressure increase due to humidity.

Table 5. Overpressure due to heating.

T (°C)	Δ*p* (bar)
25	0
600	1.9
700	2.3
800	2.6
900	2.9

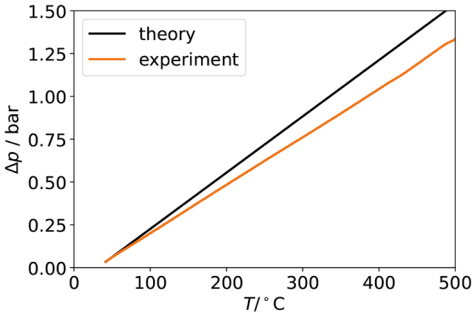

Figure 6. Pressure rise predicted by the ideal gas law (black) and measured in a battery experiment (orange).

4.5.2 Vapour pressure. The vapour pressures of Na, Zn and $ZnCl_2$ are considerable and lead to continuous evaporation in open cells – as shown exemplary in Figure 7. However, their contributions to the overall cell pressure can safely be neglected, as shown in Table 6.

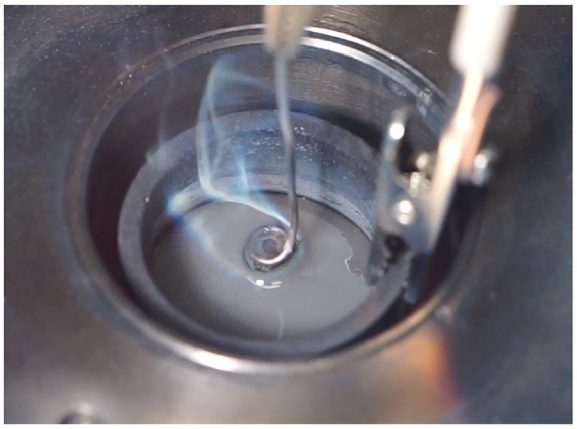

Figure 7. Na vapour forming at the anode of an open Na-Zn cell experiment.

Table 6. Vapour pressure of battery materials at 600 °C. ★ Emons *et al.*[143] do not mention the unit of their vapour pressure equation; for plausibility reasons, torr was assumed. FactSage gives an order of magnitude smaller value of $3.1 \cdot 10^{-7}$ Pa.

compound	vapour pressure		comment
	Pa	bar	
Ba	7.1	$7.1 \cdot 10^{-5}$	at melting point[45]
Ca	218	$2.2 \cdot 10^{-3}$	at melting point[45]
K	20314	0.2	[45]
Li	7.4	$7.4 \cdot 10^{-5}$	[45]
Na	3382	0.034	[144]
Sr	7.7	$7.7 \cdot 10^{-5}$	[145]
Zn	1489	0.015	[46]
$BaCl_2$	3.8	$3.8 \cdot 10^{-5}$	at melting point[146]
$CaCl_2$	0.028	$2.8 \cdot 10^{-7}$	at melting point[147]
KCl	51.5	$5.2 \cdot 10^{-4}$	at melting point[70]
LiCl	3.9	$3.9 \cdot 10^{-5}$	at melting point[147]
NaCl	46	$4.6 \cdot 10^{-4}$	at melting point[147]
$SrCl_2$	0.48	$4.8 \cdot 10^{-6}$	at melting point[143,146]★
$ZnCl_2$	16000	0.16	[70]
H_2O	$22 \cdot 10^{-6}$ Pa	220	at critical temperature of 374 °C[39]

4.5.3 Water, hydroxide and oxide decomposition. Humidity in the cell will result in hydrogen production thus increasing cell pressure. The exact amount of water depends on the cleaning of the battery parts, on the specific salt and its drying procedure. Especially ceramic parts can absorb water and should be carefully dried before use. Table 7 gives an overview of measured water contents in various salts after purification.

A water concentration of 0.3 wt% in $CaCl_2$ can be assumed as realistic while NaCl might be assumed to be fully dry. After assembling a cell in a discharged state using Zn, NaCl and $CaCl_2$, humidity might react slowly with Zn to form H_2 and $Zn(OH)_2$ as this is the stable species at room temperature – see Table 15. When heating the battery, the reaction might accelerate, forming ZnO instead of hydroxide above 85 °C[41]. During the first charge, water may alternatively react with $ZnCl_2$ (by hydrolysis) or with Na to form NaOH.

To estimate the pressure increase due to hydrogen release, only the free space above the crucible – ignoring the feedthroughs, barrel connectors and small tube – is assumed as free gas volume as

$$V = \frac{\pi}{4} d^2 h = \frac{\pi}{4} 3.7^2 \cdot 1.39 = 15\,\mathrm{cm}^3. \quad (3)$$

Assuming that the $CaCl_2$ contains 0.3 wt% water, the total water mass is $m = 0.6 \cdot 32\,\mathrm{g} \cdot 0.003 = 0.058\,\mathrm{g}$ or $n = 0.0032\,\mathrm{mol}$. At 600 °C, the ideal gas law[39,40]

$$p = nRT/V \quad (4)$$

predicts a pressure of 1 548 kPa = 15 bar for the water vapour alone assuming that all of the initial water's hydrogen is released, and its oxygen forms oxides with negligible vapour pressure. Adding the thermal expansion of the Ar gas cushion results in a total pressure difference (between the capsule interior and normal atmospheric pressure) of almost **18 bar**. Pressure measurements made on real experimental cells report values that are substantially lower than this, supporting the efficacy of the salt drying procedures described in Section 4.4.

Based on Table 15, it is impossible to predict which oxide or hydroxide will be formed preferentially at 600 °C. Comparing only the decomposition potentials, and assuming that the species with the highest potential is the most stable, the formation of $Ca(OH)_2$ would be preferred. This might be true if $Ca(OH)_2$ does not dissolve in the salt. However, if it dissociates into Ca^{2+} and OH^- ions, the various hydroxides cannot be distinguished any more and hydroxide decomposition may occur much below the decomposition potential of $Ca(OH)_2$. Moreover, complex ions, hydroxychloride or other compounds might be formed[139,148].

Under these circumstances, and also considering that the decomposition potentials in Table 15 do not account for activities, it cannot be predicted at which potentials gas evolution

Table 7. Water content in purified salts.

salt	water content	purification steps	source
$CaCl_2$	0.3 wt%	5–7 days at 100 °C, then 225 °C for 5–7 days under vacuum	107
	0.3 wt%	850 °C under vacuum, sparging with HCl for 30 min, then Ar	107
KCl	0	400 °C	96
	0	30 h at 120 °C	109
LiCl	0.17-0.4 mol%	LiCl-KCl mixture heated for 1 h in vacuum to 480 °C	119
NaCl	0	NaCl-KCl mixture heated to 700 °C under vacuum for 15 min	119
$ZnCl_2$	11.2 %	120 °C, 32 h	109

will start. It is, however, obvious that especially oxygen would immediately back-react with any metal to oxide in closed cells. Similarly, hydrogen may back-react with oxides to hydroxides if these are more stable. The full release of all bound hydrogen can therefore be considered as the worst case scenario. In any case, oxides and humidity must absolutely be avoided as their decomposition and reaction with the cell's electroactive materials might significantly reduce its coulombic efficiency.

4.5.4 Salt decomposition. If excessively low or high inter-electrode potentials are applied to the cell the electrolyte might decompose to form metal and chlorine gas. As a worst-case scenario, 12.8 g (0.219 mol) of NaCl and 19.2 g (0.173 mol) of $CaCl_2$, fully decomposed, would result in 0.28 mol of chlorine gas. Taking a simplified large cell volume of

$$V = \frac{\pi}{4} d^2 h = \frac{\pi}{4} 3.1^2 \cdot 6 = 45\,\mathrm{cm}^3 \tag{5}$$

this corresponds to a cell pressure of

$$p = nRT/V \approx 450\,\mathrm{bar}. \tag{6}$$

Table 14 gives an overview of theoretical decomposition potentials, neglecting the species' activities. It should be emphasised that the chlorine evolution reaction will compete with the Zn oxidation reaction at charge, or with the anode current collector corrosion reaction at discharge. Gas generation might therefore be slow. Moreover, chlorine is expected to back-react immediately with any metal in the cell so that it is unlikely that large amounts of chlorine can be generated.

The attentive reader might notice that the decomposition potential of $ZnCl_2$ is with 1.6 V lower than the cell's open-circuit potential. For decomposition to occur, Zn^{2+} ions need to reach the anode current collector. However, this is impossible because they will immediately be reduced by (dissolved) Na when "approaching" the anode. $ZnCl_2$ decomposition is therefore only possible if building cells containing $ZnCl_2$ in discharged state, or when (much) Na is lost during cell operation. However, care must be taken to cycle within predetermined safe potential limits.

4.5.5 Short circuit. An instantaneous adiabatic full-cell discharge is the worst conceivable outcome of a short-circuit. The resulting temperature increase can be calculated as follows.

The extent of the reaction is limited by the amount of available Na. Assuming that the battery is charged until salt solidification (DoD = 45 %) and that the complete salt column (i.e. not just the salt below the diaphragm) participates in the reaction, the amount of Na is

$$n = \frac{m}{M} = \frac{0.4 \cdot 32\mathrm{g} \cdot 0.45}{58.44\mathrm{g/mol}} = 0.1\,\mathrm{mol}, \tag{7}$$

where m denotes the mass and M the molar mass of Na.

The enthalpy change of the cell reaction (Equation 1) can be expressed as[149]

$$\Delta H = 2 \cdot H(\mathrm{NaCl}) + H(\mathrm{Zn}) - H(\mathrm{ZnCl_2}) - 2 \cdot H(\mathrm{Na}). \tag{8}$$

As simplification we neglected the enthalpy of mixing of $NaCl/ZnCl_2$ with molten $CaCl_2$ and simply extrapolate the enthalpy of formation of liquid NaCl to 600 °C and assume an ideal solution. Such an approach is justified as the enthalpy of mixing in $NaCl\text{-}CaCl_2$ systems (< 3 kJ/mol,[150]) and $NaCl\text{-}ZnCl_2$ systems (< 8 kJ/mol,[151]) indeed is small. Using the values of Table 8, the total enthalpy liberated by the reaction is then given as

$$Q = -n \cdot \Delta H = 36.5\,\mathrm{kJ}. \tag{9}$$

Table 8. Enthalpies of formation of Na, Zn and their chlorides at 600 °C.

compound	H (J/mol)	source
Na(l)	19853	41
$ZnCl_2$(l)	-356844	152
NaCl(l)	-352778	152
Zn(l)	23828	41

Considering that all $ZnCl_2$ disappears during the reaction, metallic Zn (being the most volatile constituent) would be the first to evaporate when reaching 907 °C – see Table 10. With the heat capacity of the active materials of 45.9 J/K according to Table 9 the necessary heating would consume

$$Q = (907\,\mathrm{K} - 600\,\mathrm{K}) \cdot 45.9\,\mathrm{J/K} = 14.1\,\mathrm{kJ}, \quad (10)$$

which means that 22.4 kJ are left for evaporation.

In order to evaporate all Zn, an energy of 44 kJ would be required, considering that the heat of evaporation of Zn is 115 kJ/mol[45]. Therefore, roughly 50 % of the Zn might evaporate. Assuming ideal gas behaviour and using only the free volume above the crucible (Equation 3) the resulting pressure increase would amount to 1 bar, as shown in Table 5.

4.5.6 Recommendations. Table 11 summarises reasons and values for pressure increases. Obviously, it is imperative to avoid salt decomposition due to overcharge or overdischarge. Further, it is very important to carefully dry the salts, because even small quantities of residual moisture might lead to pressure buildup on the order of 18 bar. When using new salts or trialling new charging currents, a pressure monitoring is recommended. If all recommendations are followed, normal cell overpressure will be on the order of 2 bar.

4.6 Durability of housing

The cell housing protects the environment from the cell's hazardous constituents, and the cell interior from moisture and oxygen. Its long-term integrity is therefore essential. The choice of materials, design and calculations are explained in Section 6.4. In the following, possible cell failure mechanisms will be discussed.

Table 9. Mass, molar mass, amount and heat capacities of Na, NaCl and $ZnCl_2$.

	m	*M*	*n*	c_p		source
	g	g/mol	mol	J/mol K	J/K	
Zn	25	65.39	0.3823	31.4	12.00	[153]
NaCl	12.8	58.443	0.2190	67.9	14.87	[154]
$CaCl_2$	19.2	110.983	0.1730	110	19.03	[154]
sum					45.9	

Table 10. Boiling points of Zn and the salts.

	T_b (°C)	source
Zn	907	[45]
$BaCl_2$	1560	[75]
$CaCl_2$	1936	[155]
KCl	1500	[75]
LiCl	1360	[75]
NaCl	1465	[155]
$SrCl_2$	1250	[75]
$ZnCl_2$	732	[75]

Table 11. Possible pressure increase in the cells due to various effects.

effect	pressure increase (bar)	comment
vapour pressure	0.2	by $ZnCl_2$, Zn and Na
heating	2	
short-circuit	1	
water	18	assuming 0.3 wt% water in $CaCl_2$
salt decomposition	450	
overheating	1	if 300 K more

4.6.1 Corrosion. Na is able to reduce most other metals and might therefore attack ceramics, such as the Al_2O_3 of the feedthrough; this depends of course on temperature[156]. Further, it might dissolve Ag from the braze of the feedthrough in the event that sufficient amounts of Na condense there[157]. Steel and other metals will also be attacked by HCl, which is formed due to hydrolysis caused by humidity of the salts. While pure salts are not corrosive, impurities such as O_2, H_2, H^+, H_2O or OH^- can act as oxidising agents and can lead to rapid corrosion. If the gas-tight seal is broken, then a continuous inflow of the surrounding atmosphere can be expected. In such case a rapid corrosion of the housing is inevitable, as demonstrated in Figure 8 (a). In this example, the cell was not tightened on purpose. In a short time (ca. 6 h), the corrosive salt has destroyed the housing. Liquid Zn, which will – like Na – evaporate and condensate at different places within the cell housing, is able to easily dissolve steels[158–160]. An example of a Zn dissolved Inconel barrel connector is shown in Figure 8 (b). Finally, excessively high potentials might lead to electrochemical corrosion, if there is electrical contact with the part in question. Overall, an extensive cell testing and thorough understanding is necessary to be able to safely exclude internal corrosion of the cell.

The cell might not only fail due to corrosion from the inside, but also due to attack from the outside. For example, certain insulation wools contain chloride ions which are able to attack steel[161–163]. Further, HCl vapour in chemical laboratories will have a similar effect. Maybe most importantly, the feedthrough braze is usually not stable in air and will corrode slowly. According to the manufacturer, simple Ag-Cu brazes can only be used up to 350 °C in air, while Au-covered brazes might be used up to 450 °C[164]. A failure of a small feedthrough as well as corrosion of larger Ag-Cu ones are shown in Figure 8 (c).

4.6.2 Thermal shock and stresses. Volume change and thermal stresses are extremely important for cell safety. Rapid heating or cooling is especially harmful for ceramics as they conduct heat slowly and the resulting differential stresses

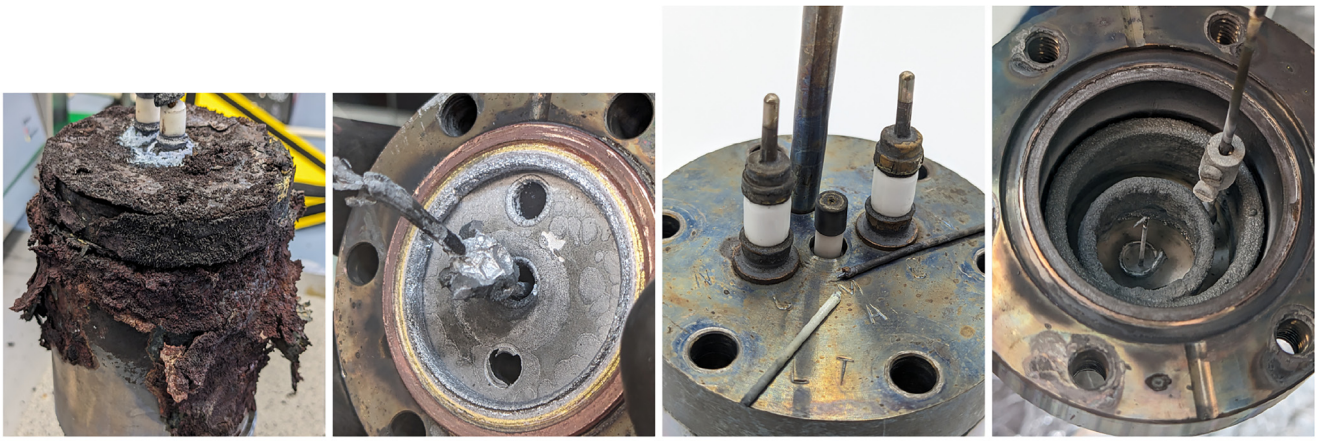

(a) (b) (c) (d)

Figure 8. Corrosion of an untight cell body due to leaked molten salts in (**a**), corrosion of an Inconel barrel connector due to Zn vapours in (**b**), failure of a small feedthrough due to high temperature and increased pressure in (**c**) and material sedimentation on internal parts leading to compositional changes and eventual failure of the cell due to high resistance in (**d**).

might lead to cracking[165]. The heating/cooling rate must therefore be limited to 5 K/min[166]. Moreover, volume change is a significant challenge as some salts expand by 20–30% upon melting – see Table 12. Zn, which melts more than 100 K earlier than the salt might be trapped in the salt and exert strong forces on its surroundings. While the battery housing has been shown to be able to cope with these stresses, the sealing of the feedthroughs might nonetheless be damaged.

4.6.3 Manufacturing defects and ageing. Weldseams can always contain defects. Although many material tests are available[167], a simple pressure test of the vessel might be the most reasonable approach to defect identification. It would also ensure that compression fittings are correctly mounted when using a pressure sensor or thermocouple. Finally, a torque wrench should be used to tighten the screws and hermetically seal the cell.

Battery ageing may be caused by any corrosion process, but also by microstructural changes in the steel from which the housing/screws are made. For example, a very brittle Fe-Cr phase might form between 600 and 800 °C if the battery is exposed to this temperature for several hours. This sigma phase can appear only in steels with a minimum Cr content of 18–20%, where Si, Mn, and Mo promote sigma phase formation[167]. As the 1.4980 steel (used here for screws) has a chromium concentration of 13.5–16%, and the 1.4306 steel (used for the housing) has chromium concentration of 18–20%, sigma phase formation is theoretically possible only for the housing.

Secondly, at 475 °C embrittlement can be expected in ferritic Cr-steels if held for several hours between a temperature of 400 and 550 °C[167]. Fortunately, this is rather improbable as the Na-Zn cell operates at higher temperature and both of the steels used are austenitic.

Finally, electrolyte ageing might be a challenge, too. As shown in Figure 8 (d), during the 400 h electrochemical cycling experiment, salt has gradually deposited on the ceramic walls, irreversibly altering the remaining composition. This eventually leads to increased resistance and higher potentials.

4.6.4 Abuse. Several possibilities exist for abuse of Na-Zn cells. Physical impacts, thermal shocks, and exposure to corrosive substances, among others, must be excluded. During disassembly, cells must be handled carefully, especially when removing their lids to avoid damage to the flange's knife-edge and/or sealing surface. The feedthroughs and pressure sensor tube in the lid are both fragile and should be handled with the necessary care. Cells should not be lifted using the pressure sensor tube.

4.6.5 Recommendations. Designing a cell housing which can safely contain the active materials under all probable circumstances is very challenging. As explained in Section 6.4 it is especially difficult to calculate the appropriate tightness of the screws at 600 °C, as well as an appropriate feedthrough design.

Cell pressures in the order of 2–3 bar during normal operation can safely be contained using the materials investigated to date (see Table 2). However, traces of moisture might induce considerable overpressure on the order of 18 bar. In such scenarios, the housing, tube and screws are still expected to maintain their integrity – most probably the braze of the feedthrough will fail first. The pressure sensor might also fail at such high pressures. Finally, volume changes leading to deformation of the current collector and stresses in the braze of the feedthrough can easily destroy the latter. Concerning long-term stability, the feedthroughs and their corrosion by air is clearly the limiting factor. Corrosion from inside is probably less problematic as long as the cell is properly sealed.

To ensure safe operation, the following safety measures are recommended:

- battery prototypes should always be operated under a fume hood as the sealing might fail at any time

Table 12. Melting points (T_m), densities (ρ) and volume change of metals and salts defined as $\Delta V/V = (V_{hot} - V_{cold})/V_{cold} = \rho_{cold}/\rho_{hot} - 1$. If no reference is given, the volume change has been calculated. ⋆ In computing the volume change of the metals, the volumetric expansion coefficient has been assumed to be 3 times the linear expansion coefficient.

substance	T_m	ρ (g/cm³)			volume change (%)		
		25 °C	T_m (lq)	600 °C	solid	melting	liquid
Ca	839[59]	1.54[40]	1.378[40]	-	4[40]⋆	7.4⋆	-
	842[40]						
Na	98[40]	0.97[40]	0.927[153,168]	0.808[153,168]	1.6[40]⋆	2.6[169]	14.7
Zn	420[40]	7.14[40]	6.574[45,46]	6.398[45]	3.8[40]⋆	4.08[169]	2.75
$BaCl_2$	962[40,59,75,98]	3.856[73,75]	3.174[40]	3.708[49]	4	3.5[70]	-
		3.91[98]					
$CaCl_2$	772[75]	2.15[75]	2.085[40]	2.091[49]	4	0.09[70]	-
	775[40]	2.174[49]					
KCl	770[59]	1.984[75]	1.527[40]	1.832[49]	8.3	17–23[70,170]	-
	771[40,98]	1.987[98]					
LiCl	605[75]	2.068[75,98]	1.502[40]	1.891[49]	9.4	26.2[170]	-
	610[40]						
	614[98]						
NaCl	801[40]	2.165[75]	1.556[40]	1.990[49]	8.8	23–30[70,170]	-
$SrCl_2$	874[40]	3.052[75,98]	2.727[40]	2.892[49]	5.5	2.4–4.2[70]	-
	875[98]						
$ZnCl_2$	283[98]	2.907[75,98]	2.54[40]	2.892[49]	3	11.6[70]	5.8[49]
	290[40,75]	2.98[49]		(at m.p.)			
$CaCl_2$-NaCl 44:56 mol %	~530[49]	2.17[49]	1.94[47]	1.91[47]	5.1[49]	5.1[49]	1.57

- only carefully dried salts should be used
- when using new salt mixtures, the cell pressure should be monitored
- standard procedures for drying, filling and assembling (torque, etc.) should be developed
- all cell prototypes need to be handled with care

5 Conclusions

A safety assessment of a Na-Zn Liquid Metal Battery (LMB) has been performed at the cell level with a focus on operation in a laboratory furnace. Material, electrical, thermal and mechanical hazards have been discussed. It has been shown that safety of Na-Zn LMBs depends crucially on the selection of a safe electrolyte; if technically possible, avoidance of LiCl and $BaCl_2$ is desirable. One of the main hazards, cell overpressure, can be avoided by proper salt purification and by operating the cell in a safe potential window, as is the case for ZEBRA, Na-S and AMBRI's Ca-Sb batteries. In terms of cell engineering, LMBs are still at a low TRL level and certain aspects of their potential failures modes are not yet fully understood. However, it can be predicted at the outset that LMBs can reach a very high safety level, similar to ZEBRA batteries, because they are not vulnerable to thermal runaway. In this important respect, the cells are safer than Na-S or Li-ion batteries, and are expected to comply with the (relatively demanding) safety standard UL 9540A[32] in future.

To further improve cell safety, a better understanding of corrosion mechanisms and corrosion products is required. The weakest components of the cell housing are the feedthroughs; here, much knowledge regarding (air-induced) corrosion, thermal stresses, and mechanical durability is missing. Finally, the extensive topic of cell design and engineering has scarcely been covered in the past and requires more attention in future. Apparently simple phenomena, like the volume change of the salt upon solidification, or thermal stresses borne by the cell housing, are crucial to operate Na-Zn cells safely and efficiently at 600 °C, but are insufficiently well understood at present. In the face of these knowledge gaps, LMB prototypes should be operated under a fume hood until the various possible failure mechanisms are fully understood. Nevertheless, continuous operation of gas-tight batteries for up to 6 weeks outside a protective environment has demonstrated that this demanding but affordable energy storage concept not only has great potential, but may also become inherently safe in the near future[28].

6 Tables and technical design specifications

6.1 Safety tests for batteries

Table 13. Typical safety tests for battery cells according to various standards[29,31,32,171,172]. For the various misuse tests, noncompliant results are, e.g. leakage, fire, explosion, release of toxic or flammable gases.

test	description
electrical tests	
overcharge	a battery is charged to 110 %
high rate charge	a battery is charged with 120 % of the specified maximal current
short circuit	a charged battery is short-circuited with max. 20 mΩ
overload under discharge	a charged battery is discharged once with 90 % of the rated overcurrent protection value of the BMS, and once with 135 % of the main fuse rating
overdischarge protection	a charged battery is discharged with the specified maximum current until the temperature/voltage protection of the BMS switches it off
temperature and operating limits	a battery is brought to specified upper temperature limit, then charged and discharged
imbalanced charging	all cells are fully discharged, while one is brought to a SoC of 50 %; then all together are charged with maximum current
insulation resistance	the electrical spacing and insulation are tested
continuity test	the grounding of the battery is tested
failure thermal management	the battery is discharged, the thermal management system switched off and the battery charged with maximum current; the same is done with discharge
working voltage measurements	the potential between live parts and metal enclosure is measured and compared with specifications
locked-rotor test	the fan of a possible cooling motor is blocked for 7 h
input current	the input current drawn by accessory devices which are connected to AC is measured
leakage current	the leakage current of AC secondary components is measured
strain relief	the strain relief of the power cord is tested
push-back relief	it is determined whether the power cord can be pushed back into the device
low voltage transformer	a possible transformer is tested for fire hazards
electromagnetic immunity tests	
electrostatic discharge	test for electrostatic contact discharge of 6 kV and air discharge of 8 kV
radio-frequency electromag. field	immunity against radio frequency is tested with 10 V/m from 80 MHz to 1 GHz and 3 V/m from 1.4 to 6 GHz

test	description
electromagnetic immunity tests	
burst immunity	immunity to electrical fast transients/bursts is tested
impulse voltage test	surges of 0.5-2 kV line-to-ground are tested which might result from lightning
radio-frequency common mode	radio-frequency conducted disturbances are tested at in- and output ports
power frequency magnetic field	immunity to 10 A/m power-frequency magnetic fields is tested
mechanical tests	
vibration	a fully charged battery is subject to random vibration
shock	a fully charged battery is subject to shock
crush	battery crushed between a fixed surface and a ribbed test platen
static force	250 N are applied on all sides at a round 30 mm surface
impact	a charged battery receives three impacts of 6.8 J
drop impact	a charged battery is dropped depending on its weight up to 1 m
wall mount fixture	an additional force of 3 times the weight of the battery is applied
hydrostatic pressure test	cell needs to support 1.5 times its hydrostatic pressure
pneumatic strength tests	cell needs to support 1.3 times its design pressure
environmental tests	
thermal cycling	environment temperature of a fully charged battery is changed between -40 and 75 °C
resistance to moisture	test of IP rating
salt fog	a salt fog test is performed for batteries to be installed near the sea
external fire exposure	a fully charged battery is subjected to a fire for 20 min and should not explode
tolerance to internal cell failure test	
single cell failure tolerance	a failing single cell should not lead to destruction of the complete battery
thermal runaway test	
cell level	a single charged cell is heated at 4-7 K/min; if thermal runaway occurs or flammable gas is released, module test follows
module level	one or several cells in a module are forced into thermal runaway to observe propagation; if thermal runaway cannot be contained in module or flammable gas is released, unit level test follows
unit level	the complete BESS is tested accounting for its installation site (indoor, outdoor)

6.2 Risk assessment table

Type of hazard	Hazard		Component	Potential consequences	Calculations done	Risk assessment Probability (P): 0 ... 100% Severity (S): 0 ... 100% P	S	Base risk	Risk reduction measures A -inherently safe design B -safeguarding C -information for use	Risk assessment after implementing risk reduction measures P	S	Residual risk
Mechanical hazards	cutting parts		any	cutting damage		30	30	60	deburring parts (A)	10	30	40
	high pressure	volume change during normal operation	-		x	10	10	20	appr. cell design (A)	5	10	15
		H2 production	due to humid assembling	-	x	40	70	110	salt drying (C)	20	70	90
			due to leakage	(see material release)		70	10	80		70	10	80
		Cl2 production	due to overcharge/overdischarge	-	x	40	100	140	definition of safe operation window (C)	20	100	120
		H2O production	due to humid material (salt)	-	x	15	70	85	salt drying (C)	5	70	75
		HCl production	due to humid material	-	x	50	60	110	salt drying (C)	20	60	80
			due to leakage	(see material release)		40	10	50	appr. cell design (A)	20	10	30
		due to heating		-	x	100	10	110	appr. cell design (A)	100	10	110
		due to overheating	caused by furnace	-	x	30	10	40	safety switchoff (A)	5	10	15
			caused by short-circuit	-	x	40	10	50	appr. cell design (A)	30	10	40
			caused by side-reaction	-		20	10	30	appr. cell design (A)	20	10	30
		due to vapour pressure			x	10	5	15		10	5	15
		due to side-reactions		-				0				0
	material release due to failing part	due to corrosion from inside	by salt	housing		30	80	110		20	80	100
				lid		30	80	110	appr. material selection (A), salt drying (C)	20	80	100
				sealing ring		30	80	110		20	80	100
				feedthrough		70	80	150		60	80	140
				crucible		20	30	50		20	30	50
			by Na (vapour)	ceramic of feedthrough		40	80	120		20	80	100
				braze of feethrough		60	80	140		10	80	90
				crucible		10	30	40		10	30	40
			by Zn (vapour)	Al2O3 or glassy carbon crucible and housing		10	30	40	appr. material selection (A)	10	30	40
				feedthrough		50	80	130		50	80	130
				sealing ring		30	80	110		30	80	110
			by HCl	metals		30	80	110	salt drying (C)	15	80	95
			by applying wrong potentials	metals		10	80	90	definition of operating window (C)	10	80	90
		due to corrosion from outside	by humidity or oxygen	housing		20	80	100		10	80	90
				lid		20	80	100		10	80	90
				feedthrough		80	80	160		80	80	160
				sealing ring		20	80	100		10	80	90
			by insulation	housing		20	80	100		10	80	90
				lid	material release, fire, injury	20	80	100	selection of appropriate materials (A)	10	80	90
				feedthrough		20	80	100		10	80	90
				sealing ring		20	80	100		10	80	90
			by chemical lab vapours (HCl)	housing		20	80	100		10	80	90
				lid		20	80	100		10	80	90
				feedthrough		20	80	100		10	80	90
				sealing ring		20	80	100		10	80	90
		due to thermal shock		feedthrough	x	80	80	160	definition of heating/cooling rate	20	80	100
				crucible		30	80	110	(C)	10	80	90
		due to manufacture	manufacturing defect	any		20	80	100		0	80	80
			bad welding	feedthrough, housing		40	80	120	pressure test (A)	0	80	80
			bad swadgelok	swadgelok		30	80	110		0	80	80
			bad torque of sealing ring	sealing ring		30	80	110	definition of safe torque (C)	10	80	90
		due to abuse	falling down	-		10	80	90		10	80	90
			lifting cell at feedthrough etc.	-		40	80	120	handling instructions (C)	10	80	90
			penetration from outside	-		10	80	90		0	80	80
		due to aging	thermal cycling	feedthrough		70	80	150		70	80	150
		due to thermal stresses	by expansion of current collector, pressing in feedthrough wire	feedthrough		80	80	160	further tests required	80	80	160
		due to overheating	(see high pressure)	-				0				0
		due to phase change		crucible				0				0
Electrical hazards	short-circuit	due to abuse		-	x	10	80	90	handling instructions (C)	10	30	40
		due to power outage		-		10	30	40		10	30	40
		due to internal short	sheat failure	sheat		80	30	110		80	30	110
			self-discharge	salt	overpressure	80	30	110		80	30	110
			bridiging electrodes by deposited Zn	cabling		80	30	110		80	30	110
			deposited Na vapour	feedthrough		60	30	90		60	30	90
	overcharge	and gas generation	and corrosion		(see high pressure)	15	90	105	definition of operating window	5	90	95
	overdischarge	and gas generation	and corrosion		(see corrosion)	15	90	105		5	90	95
	power outage				(see material release) (see short-circuit)	70	40	110		70	40	110
Thermal hazards	high temperature				burning fingers	30	30	60	instructions for use (C)	10	30	40
	outside corrosion				(see material release)			0	selection of appr. materials (A)			0
	fire					20	80	100		20	80	100
	overheating	due to failure of temperature controller			(see overpressure)	20	80	100		10	80	90
		due to removal or broken thermocouple			(see overpressure)	40	80	120		10	80	90
Radiation	infrared radiation							0				0
Material hazards	materials	active metals		Na, Zn				0				0
		co-deposited metals		Li, Ba, K, Sr, Ca				0				0
		salts		BaCl2, NaCl, ZnCl2, CaCl2, KCl, SrCl2				0				0
		structural material		alumina, alumina fibres				0				0
		corrosion products	Ni, Cr, Fe chlorides	housing				0				0
			Mo, W chlorides	currenct collector				0				0
			CuCl, CuCl2	sealing ring				0				0
			Ag, Au chlorides	feedthrough				0				0
			Oxides	humidity	(not included below)			0				0
			Hydroxides	humidity	(not included below)			0				0
	specific material hazards	skin	corrosion	alkali metals, many				0				0
			irritation	chlorides				0				0
		flammable	gas	Na, Ca, Li, Ba, K, Sr				0				0
			solid	Ba				0				0
		toxic to aquatic life		Zn, Cu, Ag, Cr, Mo chlorides				0				0
		eye	irritation	many substances				0				0
			damage					0				0
		explosive	after air contact	K-peroxide				0	Wear gloves and eye protection (C), disassembe in fumehood (C), operate under fumehood (C)			0
		harmful/toxic	if swallowed	Ba, most chlorides				0				0
			in contact with skin	CuCl2, CuCl	injury, intoxication, damage			0				0
			if inhaled	BaCl2, NiCl2, HCl, Cl2				0				0
		allergy or asthma		Au, Cr, Fe, Ni chloride				0				0
		CMR	genetic defects	NiCl2				0				0
			carcinogenic	NiCl2, ceramic fibers				0				0
		damage to unborn child		NiCl2, LiCl				0				0
		damge to organs		Ni, Cr, Mo chlorides, Cl2				0				0
		corrosive to metals		Ag, Cr, Fe, Cu chlorides				0				0
	way of exposure	aerosol	all			70	95	165		10	95	105
		vapour	Na, ZnCl2			70	95	165	Operated and disassemble under fumehood (C)	10	95	105
		gas	PH3 made from phosphorous in alumina			50	95	145		10	95	105
		skin		CuCl2		80	80	160	wear gloves (C)	10	80	90
Hazards associated with the environment	moisture				external corrosion (see material release)	10	80	90	Select appr. materials (A)	10	80	90
	fall over				(see short-circuit)	10	40	50		10	40	50
	chemical substances				(see material release)	10	30	40		10	30	40

Figure 9. Excel table of the risk assessment.

6.3 Decomposition and corrosion potentials

Decomposition potentials for many pure substances have been tabulated, and are readily available in the literature. In general, these have either been measured experimentally, or calculated from thermodynamic data (specifically, the Free energy changes of their decomposition reactions). Table 14 and Table 15 summarise such data for substances relevant to Na-Zn cells. These are substances that are either components of a prospective electrolyte, or occur as contaminants in the cell.

Table 14. Decomposition potentials of chloride salts at 600 °C. At overcharge, metal is produced on top and gas on the bottom of the cell, at overdischarge (negative potentials) inversely. Activities have been neglected.

salt	ΔE (V)	
	36	41
$BaCl_2$	3.7	3.7
$CaCl_2$	3.5	3.4
KCl	3.7	3.7
LiCl	3.6	3.5
NaCl	3.4	3.4
$SrCl_2$	3.6	3.6
$ZnCl_2$	1.6	1.5

An important caveat to the use of these tabulated values is that they are strictly valid only for pure substances, whereas a Na-Zn electrolyte comprises a solution of several substances whose components' activities may differ from their molar concentrations (i.e. exhibit non-ideal behaviour). The influence of such non-ideality on the potential is expressed by the Nernst equation, which, for a generic oxidation reaction at a single interface[173,174] is

$$E = E_0 + \frac{RT}{zF} \ln \frac{a_{ox}}{a_{red}} \quad (11)$$

where E_0 denotes the standard potential (provided by the tables), R the gas constant, F the Faraday constant, T the temperature in K, z the number of exchanged electrons, and a_{ox} and a_{red} the activities of the oxidised and reduced species respectively. The overall (inter-electrode) cell potential comprises the difference between two such interfaces

$$\Delta E = E_c - E_a \quad (12)$$

where the index a refers to the anode and c to the cathode. Thus, for the whole cell we have:

$$\Delta E = E_{0,c} - E_{0,a} + \frac{RT}{z_c F}\left(\ln a_{ox,c} - \ln a_{red,c}\right) + \frac{RT}{z_a F}\left(-\ln a_{ox,a} + \ln a_{red,a}\right). \quad (13)$$

Table 15. Decomposition potentials for oxides and hydroxides at 600 °C[41], and stability of species. At overcharge, metal is deposited on top, and gas released on bottom of the cell, at overdischarge (negative potentials) inversely. The 'stable species' entries are based on thermodynamic calculation neglecting activities and ignoring peroxides, superoxides and hydroxychlorides; the values should therefore be treated with care.

substance	product	ΔE (V)	stable species		comment
			25 °C	600 °C	
BaO $Ba(OH)_2$	Ba, O_2 H_2, O_2 H_2O, O_2 BaO, H_2O	2.4 3.6 2.6	hydroxide	hydroxide	BaO forms at 900 °C[83]
CaO $Ca(OH)_2$	Ca, O_2 H_2, O_2 H_2O, O_2 CaO, H_2O	2.8 3.80 2.76	hydroxide	oxide	2.2 V at 1000 °C[175] stability limit hydroxide is 400 °C[101,106]
K_2O KOH	K, O_2 H_2, O_2 H_2O, O_2 K_2O, H_2	1.2 3.1 2.1	hydroxide	hydroxide	KOH produced at 827 °C[110]; K_2O_2 might be more stable at 450 °C[69]

substance	product	Δ*E* (V)	stable species		comment
			25 °C	600 °C	
Li_2O LiOH	Li, O_2 H_2, O_2 H_2O, O_2 Li_2O, H_2	2.5 3.6 2.6	hydroxide	hydroxide	LiOH and Li_2O appear in comparable amount[110]; Li_2O generation starting at ~250 °C[176]
Na_2O NaOH	Na, O_2 H_2, O_2 H_2O, O_2 Na_2O, H_2O	1.5 3.1 2.1	hydroxide	hydroxide	1.76-2.18[175] NaOH produced at 450, 700[96] and 827 °C[110]
SrO $Sr(OH)_2$	Sr, O_2 H_2, O_2 H_2O, O_2 SrO, H_2	2.6 3.7 2.7	hydroxide	hydroxide	
ZnO $Zn(OH)_2$	Zn, O_2 H_2, O_2 H_2O, O_2 ZnO, H_2O	1.3 2.0 0.9	hydroxide	oxide	1.24-1.3 V[175] hydroxychlorozinc might be formed instead[139]; ZnO at least above 200 °C[134]

Evaluation of activities is non-trivial, since there is no completely general model that successfully predicts their relationship to molar concentration, and experimental measurements on halide solutions are not comprehensive. By providing only the standard state terms ($E_{0,c}$ and $E_{0,a}$), the tabulated potentials offer an approximation rather than a precise description of these decomposition potentials.

The cell potential at which one of the current-collector metals can oxidise – here termed the 'corrosion potential' – is a similarly important limit for sustainable cell operation. Table 16 displays such potentials for a range of candidate current collector metals. The metal couples in the left-hand column indicate possible exchange reactions: anode current collector versus Zn in the upper half; Na versus the cathode current collector on the lower half. The voltages displayed are those at which each metal couple undergoes electron exchange, resulting in the dissolution of the current collector metal into the electrolyte. For a pure single-component electrolyte, comprising the chloride of the reducing metal, such voltages are simply equal to the difference between the decomposition potentials of the chlorides of the metals concerned, according to Equation 12 above. However, as with the aforementioned decomposition potentials, the precise voltage for the multi-component case constituted by a Na-Zn cell, the activities of the components must be included in the calculation (Equation 13). Accordingly, Table 16 offers useful approximations rather than precise values.

6.4 Design and durability of cell

The details, calculations and further considerations concerning the cell design are summarised in this section.

6.4.1 Housing material. The steel for the cell housing needs to fulfil the following criteria:

- heat-resistance: the steel needs to maintain high strength and structural integrity when subjected to 600 °C for long periods of time
- scaling resistance: the steel needs to exhibit significant resistance to scaling, which refers to the formation of oxide layers on the surface when exposed to high temperatures in the presence of air
- long-term stability at high temperature: material degradation or structural weakening at high-temperature during long time periods needs to be prevented
- corrosion resistance: the steel needs to support the specific environment within the cell, including molten salt, Na and Zn vapour
- adequate performance under thermal changes: the material needs to support large and repeated temperature changes including expansion and contraction
- compatibility with other cell components: the steel is required to be compatible with other materials used

Table 16. Selected potentials for corrosion of current collectors.

cell	ΔE (V)		comment
	36	41	
Corrosion of anode current collector if going below			
Al-Zn	0.55	0.31	first value at 200 °C
Co-Zn	-0.47	-0.50	
Cr-Zn	-0.08	-0.06	Cr^{2+}
Cr-Zn	-0.29	-0.31	Cr^{3+}
Cu-Zn	-0.55	-0.53	Cu+
Cu-Zn	-1.05	-1.01	Cu^{2+}
Fe-Zn	-0.35	-0.31	Fe^{2+}
Fe-Zn	-0.54	-0.68	Fe^{3+}, first value at 350 °C
Mn-Zn	0.35	0.39	
Mo-Zn	-1.08	-0.69	Mo^{2+}
Mo-Zn	-1.03	-0.63	Mo^{3+}, first value at 350 °C
Mo-Zn	-0.97	-0.78	Mo^{4+}, first value at 200 °C
Ni-Zn	-0.55	-0.61	
Ti-Zn	0.33	0.41	Ti^{2+}
Ti-Zn	0.28	0.33	Ti^{3+}, first value at 500 °C
W-Zn	-1.16	-0.71	W^{2+}
W-Zn	-1.12	-0.97	W^{4+}
W-Zn	-1.16	-1.04	W^{5+}
W-Zn	-1.23	-1.10	W^{6+}
Corrosion of cathode current collector if going above			
Na-Al	1.33	1.60	
Na-Co	2.35	2.42	
Na-Cr	1.95	1.97	Cr^{2+}
Na-Cr	2.16	2.23	Cr^{3+}
Na-Cu	2.42	2.44	Cu^{+}
Na-Cu	2.92	2.93	Cu^{2+}
Na-Fe	2.22	2.22	Fe^{2+}
Na-Fe	2.41	2.60	Fe^{3+}, first value at 350 °C
Na-Mn	1.52	1.52	
Na-Mo	2.95	2.60	Mo^{2+}
Na-Mo	2.91	2.54	Mo^{3+}, first value at 350 °C
Na-Mo	2.84	2.69	Mo^{4+}, first value at 200 °C
Na-Ni	2.4	2.52	
Na-Ti	1.54	1.50	Ti^{2+}
Na-Ti	1.59	1.58	Ti^{3+}, first value at 500 °C
Na-W	3.0	2.62	W^{2+}
Na-W	2.99	2.89	W^{4+}
Na-W	3.03	2.96	W^{5+}
Na-W	3.10	3.02	W^{6+}

in the cell avoiding any adverse reactions, material incompatibilities or degradation

- manufacturing reliability: the selected steel must be consistently manufactured to precise specifications, to ensure reliability and avoid variations in material performance that could pose risks during cell operation
- weldability, if possible without pre- or postheating
- adequate machinability for easy manufacturing

Given the number of steels available in the market, it is impossible to provide clear advice how to select the most appropriate steel in a systematic manner. Even though patents of the LMB company AMBRI[177] mention 1.4016 (AISI 430)[178] to the best of our knowledge no study on suitable steels for LMBs has been published. We assume therefore that such steels which are used at high temperature for furnaces and in the chemical industry might be suitable. This includes in particular creep resistant, high-temperature steels. Table 17 provides a selection of steel grades which we consider to be suitable for LMBs.

As standard vacuum parts for our cell design were not available in the steel grades mentioned, simple 1.4306 had to be used for the housing and lid. At temperatures exceeding 500 °C, creeping will always occur[179]. We therefore base the strength calculations on the assumption that a deformation of 1 % in 10 000 h ($R_{p1.0}$) is acceptable[179]. Table 18 provides the material properties.

6.4.2 Housing cylinder. The allowed pressure within the cell housing, as dictated by its material properties, can be calculated as[180]

$$p_{al} = \frac{2R_{p1.0}S}{d_a S} = \frac{2 \cdot 138 \cdot 1.5}{40 \cdot 1.5} = 69\,\text{bar} \tag{14}$$

with $R_{p1.0}$ denoting the yield stress and S = 1.5 the safety factor[179,180]. The wall thickness is s = 1.5 mm and the outer

Table 17. Possible steels and Ni-based alloys for high-temperature batteries with an operation temperature of 600 °C.
Data taken from various material data sheets and Wegst & Wegst[181].

material	characteristics
1.4762 X10CrAlSi25 AISI 446	Ferritic stainless steel of low strength but excellent resistance to high-temperature oxidation. Weldable, but might need pre-heating. Application: industrial furnaces, combustion chambers, oil burners, heat exchangers, kiln liners, glass moulds.
1.4828 X15CrNiSi20-12 AISI 309	Standard steel in furnace building of high strength and corrosion resistance up to 650 °C in air. Weldable without preheating. Application: annealing bells, cementation and hardening boxes, annealing pots, etc. Alternatives: 1.4835, 1.4841.
1.4845 X15CrNi25-21 AISI 310S	Austenitic steel with corrosion resistance in air up to 1050 °C. Weldable. Applications: furnace building, chemical industry, steam boilers, petroleum processing plants, heat treatment baskets, etc.
1.4864 X12NiCrSi35-16 AISI 330	High strength and corrosion resistance in air up to 1000 °C. Welding without pre-heating. Applications: furnace building, chemical industry, heat exchangers.
1.4876 X10NiCrAlTi32-20 Alloy 800	High-temperature strength and excellent resistance to oxidation up to 1100 °C in air. Weldable. Applications: parts for furnace and steam boiler constructions, petroleum industry, heat exchangers, and furnace components. Similar alternatives: 1.4958 and 1.4959.
1.4910 X3CrNiMoBN17-13-3 AISI 316LN	Creep-resistant alloy for usage up to 700 °C. Weldable. Application: pressure vessels, steam boilers, chemical industry.
1.4922 X20CrMoV11-1	Creep resistant construction steel for usage in air up to 600 °C. Low corrosion resistance due to low Cr content. Application: chemical industry.
2.4816 NiCr15Fe Alloy 600	Ni-bases superalloy with excellent corrosion resistance up to 1050 °C. Weldable. Applications: industrial furnaces, chemical industry, reactors, aerospace applications.
2.4856 NiCr22Mo9Nb Alloy 625	High-temperature alloy for use up to 1050 °C with excellent corrosion resistance. Weldable without preheating. Applications: chemical process industry, offshore and environmental technology.

Table 18. Material properties of steel 1.4306 with data taken from various data sheets.

property		unit	value	comment
maximum use temperature	T_{max}	°C	600	
yield strength	$R_{p0.2}$	N/mm²	90	
yield strength	$R_{p1.0}$ (10 000 h)	N/mm²	138	for the similar 1.4307[179]
thermal expansion coefficient	α	1/K	$18 \cdot 10^{-6}$	

diameter d_a = 40 mm. As the cells will only be pressurised up to 2 bar under normal operation, the housing is safely dimensioned.

6.4.3 Tube. The tube extending through the lid capping the cell serves to connect a pressure sensor, thermocouple or similar. Using the same formula for cylindrical pressure vessels as for the cell housing, an outer diameter of 6 mm and a wall thickness 1 mm yields

$$p_{al} = \frac{2R_{p1.0}S}{d_a S} = \frac{2 \cdot 138 \cdot 1}{6 \cdot 1.5} = 307 \text{ bar}, \quad (15)$$

which is, as previous, more than sufficient to contain the expected operating pressures.

6.4.4 Compression fittings. Compression fittings are used to attach a pressure sensor, bursting disk or thermocouple to the tube. According to the manual, for a 6 mm tube, a minimum wall thickness of 0.8 mm is required[182]. With a temperature reduction factor of 0.49 for AISI 304L (1.4306), the tube would support 211 bar at 600 °C. Most probably, it can be safely assumed that the fittings are designed for the same pressure.

6.4.5 Pressure sensor. Pressure sensors are sometimes used to monitor the cell pressure during heating and to detect leaks in the housing. According to the data sheet, they support 2.5 times the pressure of their full scale[183]. The typically used 4 bar sensors can therefore only support 10 bar before they might fail.

6.4.6 Welding. The housing is TIG welded by butt joints between bottom plate and the tube, and between the tube and the flange. As these weldseams are rather thick compared to the 1.5 mm tube, no failure is expected here.

The tube in the lid as well as the feedthroughs are laser welded in order to prevent damage from the feedthroughs. As the gap between laser welded parts needs to stay below 10 % of its wall thickness, and the feedthrough tubes are only 0.5 mm thick, a maximum gap width of 0.05 mm, i.e. very narrow tolerances are required for successful welding[167]. The final weldseam is usually 1 mm wide, with its depth depending on welding speed – possibly reaching 1–5 mm[167]. Obviously an accurate machining of the parts is necessary to meet the required tolerances. As the laser welding might be imperfect, a pressure test is recommended. Laser-welded parts should be handled with care.

6.4.7 Screws and Cu sealing. The lid of the cell is fixed with six M6 screws (ISO 4017, 1.4980). The latter need to deform the Cu sealing ring sufficiently to ensure the formation of a gas-tight seal, and need to be tightened such that they do not unfasten themselves while heating. However they also need to be removable after battery cycling. Finally, they should support an internal cell pressure of 18 bar, as explained in Section 4.5.6.

The correct dimensioning of screws starts by calculation of the preload force, accounting for cell pressure, deformation of the sealing, surface pressure and deformation of parts. Knowing the required force of the screw, the torque can be calculated. Finally, the static strength, surface pressure and sealing tightness safety factors are assessed[184]. This stress analysis involves several empirical formulae, which are well established for room temperature. However, when heating the cell to 600 °C, material properties such as yield strength or elastic modulus, among others, will change. Creeping of parts will occur, since the screw, housing and Cu have different thermal expansion coefficients, as well as being subject to a temperature gradient between the hot capsule interior and the colder exterior[184,185]. Although it is very challenging to correctly design the screws under such conditions, some general statements can be made. The high-temperature material (1.4980), with its yield strength of $R_{p0.2}$ = 380 N/mm² at 650 °C[186], allows for a force of 5 880 N in each screw. This is remarkable as an internal cell pressure of 18 bar would lead only to ca. 360 N. Under some assumptions, a force of 4.5 kN per screw is required for a sufficient deformation of the sealing ring and 3 kN to keep the seal tight over time. Tightening the screws with 100 % of its yield strength would lead to 6 Nm – which is a very small value compared to typical torques for M6 at room temperature of 7.7 - 26.8 Nm[185]. As the cell housing made of 1.4306 has a lower strength, the surface pressure of order 210 N/mm² might be a problem.

Experimental trials have shown that a tightening torque of 5 Nm was not sufficient for proper sealing, and 10 Nm was hard to loosen again after a long-term cycling. Therefore, 8 Nm was identified as the appropriate average value to keep the cells gas-tight during normal cycling experiments. This

is consistent with the calculated 6 Nm – which should still be sufficient for the screws to support an internal cell pressure of 18 bar.

6.4.8 Feedthrough. The approximate dimensions of the feedthroughs used, which are acquired from Kyocera[164,166] or Alumina Systems, are shown in Figure 10. Typically, the insulator is made of Al_2O_3, the collars of Invar 42 (1.3917) and the conductor of Ni. Brazing between the ceramic and metal, as well as between the conductor and the collar is performed either with eutectic Ag-Cu braze (melting point 780 °C) or Au-Ni braze (melting point 950 °C)[164,166]. While the Ag-Cu braze is comparably cheap, it clearly reaches its limits at 600 °C – especially with small but rapid changes in temperature, the sealing will fail[28].

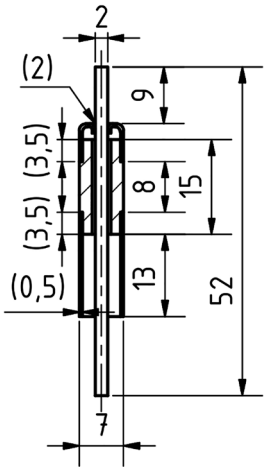

Figure 10. Dimensions of the Kyocera/Friatec feedthrough. The values in brackets are estimated from the image in the manufacturers catalogue[164].

A correct stress analysis of the feedthrough is challenging[187]. It must involve the strength of the ceramic, the thin Invar 42 collars and the three brazing points. While Invar 42 yield strengths[48] are available at 600 °C, values for the brazes are scarce[188]. Apart from the internal cell pressure, forces may act via the current collector on the pin due to different thermal expansion – as explained in Section 4.6.2. The stress conditions will be complex, and might be better addressed with FEM simulations. Applying a lateral force by, for example, attaching an off-centred current collector will add an additional strain on the braze joint. Finally, also long-term stability of materials is a challenge since the parts of the feedthroughs are susceptible to various corrosive vapours[187], e.g. Na attacks the ceramics as well as the braze while the conductive pin and collars could alloy with Zn. Cheaper Ag-Cu brazed devices are at 600 °C at their limit, and even Au-Ni brazed versions might fail if safe handling is not ensured and correct operational parameters, such as low heating/cooling rates, are not set. Overall, the sealing of the feedthrough is clearly the weakest point of the cell housing. Therefore, it is worthwhile to focus actively on improving the durability of the feedthroughs and investigating the various failure mechanisms in detail, both experimentally and numerically.

Data availability

Underlying data

The risk assessment table and selected calculations are available under the terms of the Creative Commons Attribution 4.0 International license (CC-BY 4.0)[189].

Acknowledgements

We thank the SOLSTICE consortium and especially Bernd Willers, Camilla Sommerseth, Ole Kjos, Cathrine Solem, Marta Navas, Milena Salvo and Bjarte Øye for support and helpful discussions.

References

1. Marlair G, Dupont L, Demissy M: **Approche de la maîtrise des risques spécifiques de la filière véhicules électriques.** Technical Report DRA-10-111085-11390D, INERIS, 2011.
Reference Source
2. Kabza A, Fleischhammer N, Brandt K, *et al.*: **Studie zur Bewertung der Sicherheit von Lithium-Ionen-Batterien über den gesamten Lebenszyklus.** Technical report, ZSW Ulm, 2017.
Reference Source
3. IEEE: **Guide for the ventilation and thermal management of batteries for stationary applications.** IEEE Standard 1635, 2022.
4. VDE: **Hochtemperatur-Sekundärbatterien — Teil 1: Allgemeine Anforderungen.** DIN EN IEC 62984-1, 2020.
Reference Source
5. Leonardi SG, Samperi M, Frusteri L, *et al.*: **A review of sodium-metal chloride batteries: materials and cell design.** *Batteries.* 2023; **9**(11): 524.
Publisher Full Text
6. Benato R, Sessa SD, Crugnola G, *et al.*: **Sodium-nickel chloride (Na-$NiCl_2$) battery safety tests for stationary electrochemical energy storage.** In: *2016 AEIT Int Annu Conf AEIT.* Capri, Italy, 2016; 1–5.
Publisher Full Text
7. Sudworth JL, Tilley AR, editors: **The Sodium Sulfur Battery.** Chapman and Hall, London, 1985.
Reference Source
8. Trickett D: **Current status of health and safety issues of sodium/metal chloride (Zebra) batteries.** Technical Report NREL/TP-460-25553, National Renewable Energy Laboratory, Golden, Colorado, 1998.
Reference Source
9. Armand M, Ortiz-Vitoriano N, Olarte J, *et al.*: **Salt batteries: opportunities and applications of storage systems based on sodium nickel chloride batteries.** European Union, 2023.
Reference Source
10. Benato R, Cosciani N, Crugnola G, *et al.*: **Sodium nickel chloride battery**

technology for large-scale stationary storage in the high voltage network. *J Power Sources.* 2015; **293**: 127–136.
Publisher Full Text

11. Lu X, Lemmon JP, Sprenkle V, *et al.*: **Sodium-beta Alumina batteries: status and challenges.** *J Miner Met Mater Soc.* 2010; **62**(9): 31–36.
Publisher Full Text

12. Dustmann CH: **Advances in ZEBRA batteries.** *J Power Sources.* 2004; **127**(1–2): 85–92.
Publisher Full Text

13. Chatwin T: **Abuse testing of Sodium Nickel Chloride batteries.** In: *Intelec 2013; 35th International Telecommunications Energy Conference, SMART POWER AND EFFICIENCY.* Hamburg, Germany, 2013; 318–323.
Reference Source

14. Sudworth JL: **The sodium/sulphur battery.** *J Power Sources.* 1984; **11**(1–2): 143–154.
Publisher Full Text

15. Ohi JM: **Environmental, health, and safety issues of sodium-sulfur batteries for electric and hybrid vehicles.** Technical Report NREL/TP-262-4678, National Renewable Energy Laboratory, Golden, Colorado, 1992.
Reference Source

16. Kim H, Boysen DA, Newhouse JM, *et al.*: **Liquid metal batteries: past, present, and future.** *Chem Rev.* 2013; **113**(3): 2075–2099.
PubMed Abstract | Publisher Full Text

17. Stefani F, Weier T, Gundrum T, *et al.*: **How to circumvent the size limitation of liquid metal batteries due to the Tayler instability.** *Energy Convers Manag.* 2011; **52**(8–9): 2982–2986.
Publisher Full Text

18. Kelley DH, Weier T: **Fluid mechanics of liquid metal batteries.** *Appl Mech Rev.* 2018; **70**(2): 020801.
Publisher Full Text

19. Chum HL, Osteryoung RA: **Review of thermally regenerative electrochemical cells.** Number SERI/TR-332-416. Solar Energy Research Institute, 1981.
Reference Source

20. Bradwell DJ: **Liquid metal batteries: ambipolar electrolysis and alkaline earth electroalloying cells.** PhD thesis, Massachusetts Institute of Technology, 2011.
Reference Source

21. Agruss B, Karas HR, Decker VL: **Design and development of a liquid metal fuel cell.** Technical Report ASD-TDR-62-1045, General Motors Corporation, 1962.
Reference Source

22. Agruss B, Karas HR: **First quarterly technical progress report on design and development of a liquid metal cell for the period 1 January 1962 – 31 March 1962.** Technical Report AD 274 197, Armed Service Technical Information Agency, 1962.

23. Kim J: **Cell design/fabrication and optimization of cell components for rechargeable all-liquid metal batteries.** Master thesis, Ulsan National Institute of Science and Technology, 2017.
Reference Source

24. Cairns EJ, Gay EC, Kolba VM, *et al.*: **Lithium/Selenium secondary cells for components in electric vehicular-propulsion generating systems.** Technical Report Project Order No. MERDC 175-69, Argonne National Laboratory, 1970.

25. Gay EC, Arntzen JD, Cairns EJ, *et al.*: **Lithium/chalcogen secondary cells for components in electric vehicular-propulsion generating systems.** Technical Report ANL-7863, Argonne National Laboratory, 1972.

26. Xu J, Kjos SO, Osen KS, *et al.*: **Na-Zn liquid metal battery.** *J Power Sources.* 2016; **332**: 274–280.
Publisher Full Text

27. Xu J, Martinez AM, Osen KS, *et al.*: **Electrode behaviors of Na-Zn liquid metal battery.** *J Electrochem Soc.* 2017; **164**(12): A2335–A2340.
Publisher Full Text

28. Sarma M, Lee J, Nash W, *et al.*: **Reusable cell design for high-temperature (600 °C) liquid metal battery cycling.** *J Electrochem Soc.* 2024; **171**(4): 040531.
Publisher Full Text

29. Underwriters Laboratories: **Standard for safety. Energy Storage Systems and Equipment.** UL 9540, 2023.

30. VDE: **Hochtemperatur-Sekundärbatterien - Teil 2: Sicherheitsanforderungen und Prüfungen.** DIN EN IEC 62984-2, 2021.
Reference Source

31. Underwriters Laboratories: **Standard for safety. Batteries for use in stationary and motive auxiliary power applications**. UL 1973: 2022.
Reference Source

32. Underwriters Laboratories: **Test method for evaluating thermal runaway fire propagation in battery energy storage systems**. UL 9540A: 2019.
Reference Source

33. Ara Ake: **Stationary battery energy storage systems analysis: a focus on intraday shifting**. Technical report. Ara Ake, 8 Young Street, New Plymouth 4310, 2023.
Reference Source

34. **Safety of machinery — general principles for design — risk assessment and risk reduction**. ISO 12100, 2010.
Reference Source

35. **Sicherheit von Maschinen - Risikobeurteilung - Teil 2: Praktischer Leitfaden und Verfahrensbeispiele**. DIN ISO/TR 14121, 2013.
Reference Source

36. Hamer WJ, Malmberg MS, Rubin B: **Theoretical electromotive forces for cells containing a single solid or molten chloride electrolyte.** *J Electrochem Soc.* 1956; **103**(1): 8–16.
Publisher Full Text

37. Temkin M: **Mixtures of fused salts as ionic solutions.** *Acta Physicochim. URSS,* 1945; **20**(4): 411–420.

38. Fellner P: **Comments on some models of molten salt mixtures.** *Chem Pap.* 1983; **37**: 609–615.
Reference Source

39. Stephan P, Kabelac S, Kind M, editors, *et al.*: **VDI-Wärmeatlas**. Springer Reference Technik. Springer, Berlin, Heidelberg, 2019.
Publisher Full Text

40. Lide DR, editor: **CRC handbook of chemistry and physics**. CRC Press, Boca Raton, 2005.
Reference Source

41. Roine A: **HSC chemistry**. Metso, 2023.
Reference Source

42. Auerkari P: **Mechanical and physical properties of engineering alumina ceramics**. Technical report 1792. Technical Research Centre of Finland (VTT), Espoo, 1996.
Reference Source

43. Ginnings DC, Furukawa GT: **Heat capacity standards for the range 14 to 1200 °K.** *J Am Chem Soc.* 1953; **75**(3): 522–527.
Publisher Full Text

44. Kennedy MW, Zhang K, Fritzsch R, *et al.*: **Characterization of ceramic foam filters used for liquid metal filtration.** *Metall Mater Trans B.* 2013; **44**(3): 671–690.
Publisher Full Text

45. Iida T, Guthrie RIL: **The thermophysical properties of metallic liquids**. Oxford University Press, United Kingdom, 2015.
Reference Source

46. Smithells CJ, Gale WF, Totemeier TC: **Smithells metals reference book**. Elsevier Butterworth-Heinemann, Amsterdam, 8th edition, 2004.
Reference Source

47. Janz GJ, Tomkins RPT, Allen CB, *et al.*: **Molten salts: Volume 4, part 2, chlorides and mixtures—electrical conductance, density, viscosity, and surface tension data.** *J Phys Chem Ref Data.* 1975; **4**: 871–1178.
Publisher Full Text

48. Special Metals: **The NILO® and NILOMAG® Nickel-Iron alloys**.
Reference Source

49. Bale CW, Bélisle E, Chartrand P, *et al.*: **FactSage thermochemical software and databases, 2010–2016.** *Calphad.* 2016; **54**: 35–53.
Publisher Full Text

50. DGUV: **GESTIS substance database: information system on hazardous substances of the German social accident insurance**. 2023.
Reference Source

51. Hommel G: **Merkblätter 1–414**. Springer, Berlin, Heidelberg, 1993.
Reference Source

52. National Research Council: **Prudent practices in the laboratory: handling and management of chemical hazards.** National Academies Press, Washington, D.C., 2011.
Reference Source

53. Ladge C, Beauchamp F, Bonhomme T: **French sodium school – sodium technology and sodium loop operation**. 2018.

54. Guidez J: **Phénix: the experience feedback**. EDP Sciences, Les Ulis, 2013.
Reference Source

55. Mundy CJ, Hutter J, Parrinello M: **Microsolvation and chemical reactivity of sodium and water clusters.** *J Am Chem Soc.* 2000; **122**(19): 4837–4838.
Publisher Full Text

56. Schröder V: **Explosionsgrenzen von Wasserstoff und Wasserstoff/ Methangemischen**. Technical Report 253. Bundesanstalt für Materialforschung und -prüfung, Berlin, 2002.

57. Ogden JM: **Prodspects for building a hydrogen energy infrastructure.** *Annu Rev Energy Environ.* 1999; **24**(1): 227–279.
Publisher Full Text

58. Ladwig TH: **Industrial fire prevention and protection**. Van Nostrand Reinhold, New York, 1991.
Reference Source

59. Kirk-Othmer: editor. **Kirk-Othmer encyclopedia of chemical technology**. Wiley, 2001.

60. ECHA: **Opinion proposing harmonised classification and labelling at EU level of lithium carbonate [1] lithium chloride [2] lithium hydroxide [3]**. Technical Report CLH-O-0000007034-82-01/F. European Chemicals Agency, 2021.
Reference Source

61. United Nations: **Globally Harmonized System of Classification and Labelling of Chemicals (GHS).** United Nations Publication. United Nations, New York Geneva, 2021.
Reference Source

62. Vale A, Bradberry S, Proudfoot A: **Clinical toxicology of insecticides**. In: Tim Marrs, editor. *Mammalian Toxicology of Insecticides.* The Royal Society of Chemistry, 2012; 312–347.
Publisher Full Text

63. Bumbrah GS, Krishan K, Kanchan T, *et al.*: **Phosphide poisoning: a review of literature.** *Forensic Sci Int.* 2012; **214**(1–3): 1–6.
PubMed Abstract | **Publisher Full Text**

64. AGS: **Verzeichnis krebserzeugender, erbgutverändernder oder fortpflanzungsgefährdender Stoffe**. TRGS 905, 2005.
Reference Source

65. IEEE: **IEEE recommended practice for stationary battery electrolyte spill containment and management**. IEEE, 2018; 1578–2018.
Publisher Full Text

66. ISO: **Ergonomie der thermischen Umgebung - Bewertungsverfahren für menschliche Reaktionen bei Kontakt mit Oberflächen - Teil 1: Heiße Oberflächen**. 2008. DIN EN ISO 13732-1.

67. Zieger P, Väisänen O, Corbin JC, *et al.*: **Revising the hygroscopicity of inorganic sea salt particles.** *Nat Commun.* 2017; **8**(1): 15883.
PubMed Abstract | **Publisher Full Text** | **Free Full Text**

68. Wernecke R, Wernecke J, editors: **Industrial Moisture and Humidity Measurement.** Wiley-VCH, Weinheim, Germany, 2014.

69. Inman D, Lovering DG, editors: **Ionic Liquids.** Springer US, Boston, MA, 1981.
Publisher Full Text

70. Janz GJ: **Molten Salts Handbook.** Academic Press, New York, London, 1967.
Publisher Full Text

71. Williams DF: **Assessment of Candidate Molten Salt Coolants for the NGNP/NHI Heat-Transfer Loop**. Technical Report ORNL/TM-2006/69, Oak Ridge National Laboratory, 2006.
Reference Source

72. Gardner HJ, Brown CT, Janz GJ: **The preparation of dry alkali chlorides for solutes and solvents in conductance studies.** *J Phys Chem.* 1956; **60**(10): 1458–1460.
Publisher Full Text

73. Ropp RC: **The Alkaline Earths as Metals.** In: *Encyclopedia of the Alkaline Earth Compounds.* Elsevier, 2013; 1–23.
Publisher Full Text

74. Holleman AF, Wiberg N: **Lehrbuch der anorganischen Chemie.** Walter de Gruyter, Berlin, New York, 2007.
Publisher Full Text

75. Patnaik P: **Handbook of Inorganic Chemicals.** McGraw-Hill, New York, 2003.
Reference Source

76. Mellor JW: ***Cu, Ag, Au, Ca, Sr, Ba.* Number III in A Comprehensive Treatise on Inorganic and Theoretical Chemistry**. Longmans, Green and Co. Ltd., 1922.

77. Fenstad J, Fray DJ: **The binary diagram water+barium chloride.** *C R Chim.* 2006; **9**(10): 1235–1242.
Publisher Full Text

78. Benrath A, Lechner K: **Das reziproke Salzpaar $CdCl_2$+$BaBr_2$=$CdBr_2$+$BaCl_2$.** *Z für anorg allg Chem.* 1940; **244**(4): 359–376.
Publisher Full Text

79. Assarsson G: **Equilibria in the ternary system $MgCl_2$-$BaCl_2$-H_2O between 18 and 100°.** *J Phys Chem.* 1956; **60**: 1436–1439.

80. Duval C: **Inorganic Thermogravimetric Analysis.** Elsevier, Amsterdam, London, New York, 1963.

81. Lumpkin JA, Perlmutter D: **Thermal and water vapor effects on the rate of the dehydration reactions of barium chloride.** *Thermochim Acta.* 1995; **249**: 335–349.
Publisher Full Text

82. Ekberg C, Brown PL: **Hydrolysis of metal ions**. WILEY-VCH, Weinheim, Germany, 2016.
Publisher Full Text

83. Bellobono IR, Marcandalli B, Selli E, *et al.*: **Thermodynamic analysis of the reaction of barium chloride with water vapour from 1173 to 1473K.** *Mater Chem Phys.* 1984; **10**(2): 163–174.
Publisher Full Text

84. Baes CF, Mesmer RE: **The hydrolysis of cations**. Wiley-Interscience, New York, Sydney, London, Toronto, 1976.
Reference Source

85. Neumann B, Kröger C, Jüttner H: **Die Systeme Erdalkalichlorid-Erdalkalioxyd und die Zersetzung der Erdalkalichloride durch Wasserdampf.** *Zeitschr Elektrochem.* 1935; **41**(10): 725–736.
Publisher Full Text

86. Pátek J, Klomfar J, Součková M: **Solid-Liquid equilibrium in the system of $CaCl_2$-H_2O with special regard to the transition points.** *J Chem Eng Data.* 2008; **53**(10): 2260–2271.
Publisher Full Text

87. Schiffries CM: **Liquid-absent aqueous fluid inclusions and phase equilibria in the system $CaCl_2$-NaCl-H_2O.** *Geochim Cosmochim Acta.* 1990; **54**(3): 611–619.
Publisher Full Text

88. Li D, Zeng D, Yin X, *et al.*: **Phase diagrams and thermochemical modeling of salt lake brine systems. II. NaCl+H_2O, KCl+H_2O, $MgCl_2$+H_2O and $CaCl_2$+H_2O systems.** *Calphad.* 2016; **53**: 78–89.
Publisher Full Text

89. Ally MR: **Predicting phase diagram of the $CaCl_2$ ·H_2O binary system from the BET adsorption isotherm.** *Fluid Ph Equilib.* 2008; **268**(1–2): 45–50.
Publisher Full Text

90. Qiao C, Suraneni P, Weiss J: **Phase diagram and volume change of the $Ca(OH)_2$-$CaCl_2$-H_2O system for varying $Ca(OH)_2$/$CaCl_2$ molar ratios.** *J Mater Civ Eng.* 2018; **30**(2): 04017281.
Publisher Full Text

91. Zeng D, Xu W, Voigt W, *et al.*: **Thermodynamic study of the system ($LiCl$+$CaCl_2$+H_2O).** *J Chem Thermodyn.* 2008; **40**(7): 1157–1165.
Publisher Full Text

92. Pitzer KS, Shi Y: **Thermodynamics of calcium chloride in highly concentrated aqueous solution and in hydrated crystals.** *J Solut Chem.* 1993; **22**(2): 99–105.
Publisher Full Text

93. Pitzer KS, Oakes CS: **Thermodynamics of calcium chloride in concentrated aqueous solutions and in crystals.** *J Chem Eng Data.* 1994; **39**(3): 553–559.
Publisher Full Text

94. Molenda M, Bouché M, Linder M, *et al.*: **Thermochemical energy storage for low temperature applications: materials and first studies in a gas-solid reactor.** In: *International Conference on Energy Storage*. 2012; 1–10.
Reference Source

95. Mellor JW: ***Ra and Ac Families, Be, Mg, Zn Cd, Hg.* Number IV in a comprehensive treatise on inorganic and theoretical chemistry.** Longmans, Green and Co. Ltd., 1929.
Reference Source

96. Smith DM, Neu MP, Garcia E, *et al.*: **Hydration of plutonium oxide and process salts, NaCl, KCl, $CaCl_2$, $MgCl_2$: effect of calcination on residual water and rehydration.** *Waste Manag.* 2000; **20**: 479–490.
Publisher Full Text

97. Meisingset KK, Gronvold F: **Thermodynamic properties and phase transitions of salt hydrates between 270 and 400 K IV. $CaCl_2$ ·$6H_2O$, $CaCl_2$ ·$4H_2O$, $CaCl_2$ ·$2H_2O$, and $FeCl_3$ ·$6H_2O$.** *J Chem Thermodyn.* 1986; **18**: 159–173.
Publisher Full Text

98. Wiley VCH, editor: **Ullmann's encyclopedia of industrial chemistry.** Wiley, 2007.

99. Molenda M, Stengler J, Linder M, *et al.*: **Reversible hydration behavior of $CaCl_2$ at high H_2O partial pressures for thermochemical energy storage.** *Thermochim Acta.* 2013; **560**: 76–81.
Publisher Full Text

100. Bischoff JL, Rosenbauer RJ, Fournier RO: **The generation of HCI in the system $CaCl_2$-H_2O: vapor-liquid relations from 380-500 ◦ C.** *Geochim Cosmochim Acta.* 1996; **60**(1): 7–16.
Publisher Full Text

101. Gonzalez M, Faulkner E, Zhang C, *et al.*: **Electrochemical methods for analysis of hydroxide and oxide impurities in Li, Mg/Na, and Ca based molten chloride salts.** *ECS Trans.* 2020; **98**(10): 161–169.
Publisher Full Text

102. Tomkute V, Solheim A, Olsen E: **CO_2 capture by CaO in molten CaF_2-$CaCl_2$: optimization of the process and cyclability of CO_2 capture.** *Energy Fuels.* 2014; **28**(8): 5345–5353.
Publisher Full Text

103. Kondo H, Asaki Z, Kondo Y: **Hydrolysis of fused calcium chloride at high temperature.** *Metall Trans B.* 1978; **9**(3): 477–483.
Publisher Full Text

104. Olsen E, Hansen M, Nygård HS: **Hydrolysis of molten $CaCl_2$-CaF_2 with additions of CaO.** *AIMS Energy.* 2017; **5**(6): 873–886.
Publisher Full Text

105. Vainio E, DeMartini N, Hupa L, *et al.*: **Hygroscopic properties of calcium chloride and its role on cold-end corrosion in biomass combustion.** *Energy Fuels.* 2019; **33**(11): 11913–11922.
Publisher Full Text

106. Natsui S, Shibuya R, Suzuki RO, *et al.*: **Quantification of the impact of residual H_2O on cathodic behavior in molten $CaCl_2$ electrolysis.** *J Sustain Metall.* 2022; **8**(1): 532–540.
Publisher Full Text

107. Fife KW, Bowersox DF, Christensen DC, *et al.*: **The preparation of fused chloride salts for use in pyro-chemical plutonium recovery operations at los alamos.** Technical Report LA-10681, Los Alamos National Laboratory, 1986.
Reference Source

108. Huguet L, Barge-Zwick V, Bars ML: **Dynamics of a reactive spherical particle falling in a linearly stratified fluid.** *Phys Rev Fluids.* 2020; **5**(11): 114803.
Publisher Full Text

109. Wang X, Hu Q, Kim GP, *et al.*: **Experimental study of the hygroscopy of single and different mixtures of $MgCl_2$, KCl, NaCl, ZnC_2 for application as heat transfer fluid in CSP.** In: *Proc ASME.* Pittsburgh, 2018; 1–10.
Publisher Full Text

110. Smirnov MV, Korzun IV, Oleynikova VA: **Hydrolysis of molten alkali chlorides, bromides and iodides.** *Electrochim Acta.* 1988; **33**(6): 781–788.
Publisher Full Text

111. Johnson CR: **Hydrolysis of alkali chlorides.** *J Phys Chem.* 1935; **39**(6): 791–796.
Publisher Full Text

112. Briner E, Roth P: **Recherches sur l'hydrolyse par la vapeur d'eau de chlorures alcalins seuls ou additionnés de divers adjuvants.** *Helv Chim Acta.* 1948; **31**(5): 1352–1360.
PubMed Abstract | **Publisher Full Text**

113. Sohr J, Schmidt H, Voigt W: **Higher hydrates of lithium chloride, lithium**

bromide and lithium iodide. *Acta Crystallogr C Struct Chem.* 2018; **74**(Pt 2): 194–202.
PubMed Abstract | Publisher Full Text

114. Monnin C, Dubois M, Papaiconomou N, *et al.*: **Thermodynamics of the LiCl + H_2O System.** *J Chem Eng Data.* 2002; **47**(6): 1331–1336.
Publisher Full Text

115. Li D, Zeng D, Han H, *et al.*: **Phase diagrams and thermochemical modeling of salt lake brine systems. I. LiCl+H_2O system.** *Calphad.* 2015; **51**: 1–12.
Publisher Full Text

116. Pátek J, Klomfar J: **Solid-liquid phase equilibrium in the systems of LiBr-H_2O and LiCl-H_2O.** *Fluid Phase Equilib.* 2006; **250**(1–2): 138–149.
Publisher Full Text

117. Kamali AR, Fray DJ, Schwandt C: **Thermokinetic characteristics of lithium chloride.** *J Therm Anal Calorim.* 2011; **104**(2): 619–626.
Publisher Full Text

118. Masset PJ: **Thermogravimetric study of the dehydration reaction of LiCl·H_2O.** *J Therm Anal Calorim.* 2009; **96**(2): 439–441.
Publisher Full Text

119. Burkhard WJ, Corbett JD: **The solubility of water in molten mixtures of LiCl and KCl.** *J Am Chem Soc.* 1957; **79**(24): 6361–6363.
Publisher Full Text

120. Laitinen HA, Ferguson WS, Osteryoung RA: **Preparation of pure fused lithium chloride-potassium chloride eutectic solvent.** *J Electrochem Soc.* 1957; **104**(8): 516.
Publisher Full Text

121. Swain L, Ghosh S, Pakhui G, *et al.*: **Redox behavior of Moisture in LiCl-KCl eutectic melts: a cyclic voltammetry study.** *Nucl Technol.* 2021; **207**(1): 119–146.
Publisher Full Text

122. Anderko A, Pitzer KS: **Phase equilibria and volumetric properties of the systems KCl-H_2O and NaCl-KCl-H_2O above 573K: equation of state representation.** *Geochim Cosmochim Acta.* 1993; **57**(20): 4885–4897.
Publisher Full Text

123. Niazi S, Nygård HS, Reis B, *et al.*: **Consistent thermodynamic modeling of H_2O-HCl-KOH-KCl between 200 K and 1,000 K.** *Chem Eng Sci.* 2022; **264**: 118209.
Publisher Full Text

124. Steiger M: **Thermodynamic properties of $SrCl_2$(aq) from 252 K to 524 K and phase equilibria in the $SrCl_2$-H_2O system: implications for thermochemical heat storage.** *J Chem Thermodyn.* 2018; **120**: 106–115.
Publisher Full Text

125. Clark RJ, Farid M: **Hydration reaction kinetics of $SrCl_2$ and $SrCl_2$-cement composite material for thermochemical energy storage.** *Sol Energy Mater Sol Cells.* 2021; **231**: 111311.
Publisher Full Text

126. Blijlevens MAR, Mazur N, Kooijman W, *et al.*: **A study of the hydration and dehydration transitions of $SrCl_2$ hydrates for use in heat storage.** *Sol Energy Mater Sol Cells.* 2022; **242**: 111770.
Publisher Full Text

127. Gavini SN, Vyas SN: **Solvents effects on solubility and dehydration of strontium chloride.** *J Chem Eng Data.* 1979; **24**(4): 258–261.
Publisher Full Text

128. Tanaka H, Shimada S, Negita H: **The kinetic study of thermal dehydration stages of $SrCl_2 \cdot 2H_2O$ and its deuterium analog.** *Int J Chem Kinet.* 1985; **17**(2): 149–156.
Publisher Full Text

129. Follner H, Brehler B: **Die Kristallstruktur des $ZnCl_2$·4/3H_2O.** *Acta Cryst.* 1970; **B26**: 1679–1682.
Publisher Full Text

130. Pillai SB, Wilcox RJ, Hillis BG, *et al.*: **Understanding the water-in-salt to salt-in-water characteristics across the Zinc Chloride: water phase diagram.** *J Phys Chem B.* 2022; **126**(11): 2265–2278.
PubMed Abstract | Publisher Full Text

131. Hennings E, Schmidt H, Voigt W: **Crystal structures of $ZnCl_2$·2.5H_2O, $ZnCl_2$·3H_2 and $ZnCl_2$·4.5H_2O.** *Acta Crystallogr Sect E Struct Rep Online.* 2014; **70**(Pt 12): 515–518.
PubMed Abstract | Publisher Full Text | Free Full Text

132. Wilcox RJ, Losey BP, Folmer JCW, *et al.*: **Crystalline and liquid structure of Zinc Chloride trihydrate: a unique Ionic liquid.** *Inorg Chem.* 2015; **54**(3): 1109–1119.
PubMed Abstract | Publisher Full Text

133. Kirilenko IA: **Glass formation in the $ZnCl_2$-H_2O system.** *Russ J Inorg Chem.* 2013; **58**(10): 1183–1186.
Publisher Full Text

134. Jones F, Tran H, Lindberg D, *et al.*: **Thermal stability of zinc compounds.** *Energy Fuels.* 2013; **27**(10): 5663–5669.
Publisher Full Text

135. Threlfall R: **The electrolysis of molten Zinc Chloride.** *J Soc Chem Ind.* 1929; **48**(30).
Publisher Full Text

136. Niazi S: **Experimental and theoretical evaluation of thermodynamic properties of low melting chlorides suitable for liquefaction of biomass**. PhD thesis, Norwegian University of Life Sciences, 2022.
Reference Source

137. Watson RF, Perry GS: **Solubility of ZnO and hydrolysis of $ZnCl_2$ in KCI melts.** *J Chem Soc Faraday Trans.* 1991; **87**(18): 2955–2960.
Publisher Full Text

138. Niazi S, Olsen E, Nygård HS: **Hydrolysis of eutectic compositions in the $ZnCl_2$: KCl:NaCl ternary system and effect of adding ZnO.** *J Mol Liq.* 2020; **317**: 114069.
Publisher Full Text

139. Hamilton HGC: **Hydrolytic and associated reactions in molten zinc chloride-sodium chloride**. PhD thesis, Imperial College of Science, Technology and Medicine, London, 1989.

140. Bloom H, Welch BJ: **The vapor pressure of cadmium and zinc chlorides.** *J Phys Chem.* 1958; **62**(12): 1594–1595.
Publisher Full Text

141. Keneshea FJ, Cubicciotti D: **Vapor pressures of zinc chloride and zinc bromide and their gaseous dimerization.** *J Chem Phys.* 1964; **40**(1): 191–199.
Publisher Full Text

142. **Richtlinie 2014/68/EU des Europäischen Parlaments und des Rates vom 15. Mai 2014 zur Harmonisierung der Rechtsvorschriften der Mitgliedstaaten über die Bereitstellung von Druckgeräten auf dem Markt**. Directive 2014/68/EU. 2014.
Reference Source

143. Emons HH, Bräutigam G, Thomas R: **Dampfdruckmessungen an binären geschmolzenen Mischungen aus Erdalkalimetall- und Alkalimetallchloriden.** *Chem Zvesti.* 1976; **30**(6): 773–782.

144. International Atomic Energy Agency: **Thermophysical properties of materials for nuclear engineering: a tutorial and collection of data**. International Atomic Energy Agency, Vienna, 2008.
Reference Source

145. Boerboom AJH, Reyn HW, Kistemaker J: **Heat of sublimation and vapour pressure of strontium.** *Physica.* 1964; **30**(1): 254–257.
Publisher Full Text

146. Emons HH, Kiessling D, Horlbeck W: **Dampfdruckmessungen und massenspektrometrische Untersuchungen der Gasphase über Erdalkalimetallhalogeniden.** *Z Für Anorg Allg Chem.* 1982; **488**(1): 219–222.
Publisher Full Text

147. Janz GJ, Allen CB, Bansal NP, *et al.*: **Physical properties data compilations relevant to energy storage. II. molten salts: Data on Single and Multi-Component Salt Systems**. U. S. Department of Commerce, Troy, New York, 1979.
Reference Source

148. Hoffman JW, Lauder I: **Basic Zinc Chlorides.** *Aust J Chem.* 1968; **21**(6): 1439–1443.
Publisher Full Text

149. Reid CE: **Chemical thermodynamics**. McGraw-Hill, New York, 1990.
Reference Source

150. Emons HH, Voigt W: **Zur Chemie geschmolzener Salze**. Akademie-Verlag, 1981.
Publisher Full Text

151. Manga VR, Bringuier S, Paul J, *et al.*: **Molecular dynamics simulations and thermodynamic modeling of NaCl–KCl–$ZnCl_2$ ternary system.** *Calphad.* 2014; **46**: 176–183.
Publisher Full Text

152. Romero-Serrano A, Hernandez-Ramirez A, Cruz-Ramirez A, *et al.*: **Optimization and calculation of the MCl–$ZnCl_2$ (M=Li, Na, K) phase diagrams.** *Thermochim Acta.* 2010; **510**(1–2): 88–92.
Publisher Full Text

153. Iida T, Guthrie RIL: **The physical properties of liquid metals**. Oxford Science Publications. Clarendon Press, Oxford, 1988.
Reference Source

154. Redkin AA, Zaykov YP: **Relation between the thermal expansion coefficient and the heat capacity in halide melts.** *Russ Metall Met.* 2017; **2017**(2): 75–78.
Publisher Full Text

155. Lide DR, editor: **CRC handbook of chemistry and physics: a ready-reference book of chemical and physical data**. CRC Press, Boca Raton, Fla., 1995.
Reference Source

156. Meisel P: **Werkstoffliche und technologische Entwicklungen für keramische Wärmerohre zur Hochtemperaturanwendung**. PhD thesis, Technische Universität Dresden, 2016.
Reference Source

157. Pelton AD: **The Ag-Na (Silver-Sodium) system.** *Bull Alloy Phase Diagr.* 1986; **7**(2): 133–136.
Publisher Full Text

158. Ma S, Xing J, Fu H, *et al.*: **Interfacial morphology and corrosion resistance of Fe–B cast steel containing chromium and nickel in liquid zinc.** *Corros Sci.* 2011; **53**(9): 2826–2834.
Publisher Full Text

159. Xu J, Bright MA, Liu X, *et al.*: **Liquid metal corrosion of 316l stainless steel, 410 stainless steel, and 1015 carbon steel in a molten zinc bath.** *Metall Mater Trans A.* 2007; **38**(11): 2727–2736.
Publisher Full Text

160. Han K, Ohnuma I, Okuda K, *et al.*: **Experimental determination of phase diagram in the Zn-Fe binary system.** *J Alloys Compd.* 2018; **737**: 490–504.
Publisher Full Text

161. Cammerer WF: **Wärme- und Kälteschutz**. Springer, Berlin, Heidelberg, 5th edition, 1995.
Publisher Full Text

162. Arbeitsgemeinschaft Industriebau e.V: **Mineralwolle als Dämmstoff für betriebstechnische Anlagen**. AGI Q 132, 2006.

163. Arbeitsgemeinschaft Industriebau e.V: **Calcium-Magnesium-Silikatfaster (CMS-Faser) als Dämmstoff für betriebstechnische Anlagen**. AGI Q 140, 2002.
Reference Source

164. Friatec: **Electrical feedthroughs and insulating tubes: ceramic-to-metal components**. Product catalogue, 2023.

165. Danzer R, Lube T, Supancic P, *et al.*: **Fracture of ceramics.** *Adv Eng Mater.* 2008; **10**(4): 275–298.
Publisher Full Text

166. Kyocera: **Elektro- und beschleunigertechnik. Keramik-Metall-Verbundbauteile aus Hochleistungskeramik**. Product catalogue, 2023.
Reference Source

167. GSI: **Internationaler Schweißfachingenieurlehrgang.** Gesellschaft für Schweißtechnik International mbH, 2010.

168. Sobolev V: **Database of thermophysical properties of liquid metal coolants for GEN-IV**. Technical Report SCK•CEN-BLG-1069, SCK CEN, Mol, Belgium, 2011.
Reference Source

169. Wittenberg LJ, DeWitt R: **Volume contraction during melting; emphasis on lanthanide and actinide metals.** *J Chem Phys.* 1972; **56**(9): 4526–4533.
Publisher Full Text

170. Bloom H: **The chemistry of molten salts**. W. A. Benjamin, Inc., New York, Amsterdam, 1967.
Reference Source

171. IEC: **Sicherheitsanforderungen an Sekundär-Batterien und Batterieanlagen - Teil 1: allgemeine Sicherheitsinformationen**. IEC 62485-1, 2019.
Reference Source

172. IEC: **Sicherheitsanforderungen an Sekundär-Batterien und Batterieanlagen - Teil 2: stationäre Batterien**. IEC 62485-2, 2019.
Reference Source

173. Vetter KJ: **Electrochemical kinetics**. Elsevier Science, Burlington, 1967.
Reference Source

174. Bagotsky VS: **Fundamentals of electrochemistry**. The Electrochemical Society Series. Wiley-Interscience, Hoboken, New Jersey, 2006.
Publisher Full Text

175. Delimarskii IK, Markov BF: **Electrochemistry of fused salts**. The Sigma Press, Washington, D.C., 1961.
Reference Source

176. Dinh LN, McLean II M, Schildbach MA, *et al.*: **The nature and effects of the thermal stability of lithium hydroxide.** *J Nucl Mater.* 2003; **317**(2–3): 175–188.
Publisher Full Text

177. Ambri: **Technology**. Ambri, 2019.
Reference Source

178. Thompson G, Bradwell DJ, Pujari V, *et al.*: **Ceramic materials and seals for high temperature reactive material devices**. World patent WO2016141354A2, 2022.
Reference Source

179. Informationsstelle Edelstahl Rostfrei: **Nichtrostende und hitzebeständige Stähle bei hohen Temperaturen**. Technical Report Merkblatt 987. Informationsstelle Edelstrahl Rostfrei, Düsseldorf, 2023.
Reference Source

180. Wegener E: **Festigkeitsberechnung verfahrenstechnischer Apparate**. Wiley, 2002.
Reference Source

181. Wegst C, Wegst M: **Stahlschlüssel**. Verlag Stahlschlüssel Wegst GmbH, Marbach, 20th edition, 2004.

182. Hylok: **Hy-Lok Klemmringverschraubungen**. Katalog H-200TF-D, Hy-Lok D Vertriebs GmbH, 2023.
Reference Source

183. Sensorshop24: **Drucktransmitter G1/4" oder G1/2" für Über- und Unterdruck mit Normstecker (0-10V/4-20mA)**. Product datasheet, 2023.
Reference Source

184. Muhs D, Wittel H, Jannasch D, *et al.*: **Roloff/Matek Maschinenelemente: Normung, Berechnung, Gestaltung**. Springer, Wiesbaden, 2005.
Reference Source

185. VDI: **Systematic calculation of highly stressed bolted joints - joints with one cylindrical bolt**. VDI 2230, 2015.
Reference Source

186. Valbruna: **Valbruna AN 5 / Alloy 286 / 1.4980**. Materials datasheet, 2023.
Reference Source

187. Baggio A, D'Isanto F, Valenza F, *et al.*: **The joining of alumina to hastelloy by a TiZrCuNi filler metal: wettability and interfacial reactivity.** *Materials.* 2023; **16**(5): 1976.
Publisher Full Text

188. Stephens JJ, Burchett SN, Hosking FM: **High temperature creep properties of eutectic and near eutectic silver- copper alloys: application to metal/ceramic joining**. Technical Report SAND-91-0006C; CONF-911003-10: DE91017987, Sandia National Laboratories, Albuquerque, United States, 1991.
Reference Source

189. Weber N, Duczek C, Marquez GM, *et al.*: **Data publication: risk assessment for Na-Zn liquid metal batteries**. May 2024.
Reference Source

Open Peer Review

Current Peer Review Status: ? ?

Version 1

Reviewer Report 17 December 2024

https://doi.org/10.21956/openreseurope.19170.r46066

© **2024 Liu B et al.** This is an open access peer review report distributed under the terms of the Creative Commons Attribution License, which permits unrestricted use, distribution, and reproduction in any medium, provided the original work is properly cited.

?

Binghe Liu
Chongqing University, Chongqing, China
Yue Liu
Chongqing University (Ringgold ID: 47913), Chongqing, Chongqing, China

This paper presents a systematic risk assessment covering material, electrical, thermal, and mechanical hazards. Detailed experimental methods and results are provided to help validate theoretical analyses.
1. In Figure 3, “Cell design and main dimensions” requires more details to show the names of each component.
2. How can battery components and sensors work properly at high temperatures of 600℃? Especially for porous diaphragms.
3. Add more details about the experimental setup and outcomes to support the conclusions better. For example, how exactly is overpressure measured and verified?
4. For using LiCl and BaCl2, it is recommended to discuss possible alternatives and their advantages and disadvantages.
5. Expand on how to prevent thermal runaway in Na-Zn batteries. Detailed descriptions of how the battery remains safe under various conditions would be helpful.
6. Propose specific steps to improve the technical maturity and address durability issues of Na-Zn batteries.

Is the work clearly and accurately presented and does it cite the current literature?
Yes

Is the study design appropriate and does the work have academic merit?
Yes

Are sufficient details of methods and analysis provided to allow replication by others?
Yes

If applicable, is the statistical analysis and its interpretation appropriate?

Yes

Are all the source data underlying the results available to ensure full reproducibility?
Partly

Are the conclusions drawn adequately supported by the results?
Yes

Competing Interests: No competing interests were disclosed.

Reviewer Expertise: The modelling and safety of batteries.

We confirm that we have read this submission and believe that we have an appropriate level of expertise to confirm that it is of an acceptable scientific standard, however we have significant reservations, as outlined above.

Reviewer Report 22 November 2024

https://doi.org/10.21956/openreseurope.19170.r46881

© **2024 Ahmad F.** This is an open access peer review report distributed under the terms of the Creative Commons Attribution License, which permits unrestricted use, distribution, and reproduction in any medium, provided the original work is properly cited.

?

Farooq Ahmad
nstitute of Molecular Physics Polish Academy of Sciences, Poznań, Poland

Dear authors,

I have gone through your manuscript. However, some major issues need to be fixed before I can recommend its indexing.

1. Highlight the unique advantages of Na-Zn batteries over other technologies for a stronger context.
2. Compare identified risks quantitatively with similar risks in other battery technologies.
3. Provide more details about the experimental setup and outcomes to substantiate conclusions.
4. Discuss potential alternatives to LiCl and BaCl2 and their trade-offs.
5. Suggest specific research directions to address housing durability concerns.
6. Add technical details or data to strengthen the safety comparison with ZEBRA technology.
7. Expand on mechanisms preventing thermal runaway in Na-Zn cells.
8. Outline steps to improve TRL and resolve durability issues.
9. Include environmental and health implications of hazardous aerosol release.
10. Add schematics or risk matrices to enhance the clarity of risk assessment findings.

Is the work clearly and accurately presented and does it cite the current literature?

Partly

Is the study design appropriate and does the work have academic merit?
Partly

Are sufficient details of methods and analysis provided to allow replication by others?
Yes

If applicable, is the statistical analysis and its interpretation appropriate?
Partly

Are all the source data underlying the results available to ensure full reproducibility?
Partly

Are the conclusions drawn adequately supported by the results?
Partly

Competing Interests: No competing interests were disclosed.

Reviewer Expertise: Batteries, Solid Electrolytes, Supercapacitors, and Energy Storage Devices, Electrode Materials, LiS batteries

I confirm that I have read this submission and believe that I have an appropriate level of expertise to confirm that it is of an acceptable scientific standard, however I have significant reservations, as outlined above.